Biomacromolecules

pubs.acs.org/Biomac

Perspective

PLA Block Polymers: Versatile Materials for a Sustainable Future

Daniel M. Krajovic, Margaret S. Kumler, and Marc A. Hillmyer*

Cite This: *Biomacromolecules* 2025, 26, 2761−2783

Read Online

ACCESS | Metrics & More | Article Recommendations | Supporting Information

ABSTRACT: Block polymers present an almost endless realm of possibilities to develop functional materials for myriad applications. The established self-assembly of block polymers allows researchers to access properties that are inaccessible in homopolymers. However, there is a need to develop more sustainable options than the current commodity block polymers. Derived from renewable resources and industrially compostable, poly(lactide) (PLA) is at the forefront of technological advancements in sustainable block polymers. Its material properties including high stiffness, relatively high glass transition temperature, and semicrystallinity in isotactic versions lend themselves to many applications, and its ease of synthesis provides a well-established platform for developing high-performance materials. This Perspective highlights recent advancements associated with PLA-containing block polymers, including their syntheses, mesostructural considerations, and mechanical properties, from resilient elastomers to tough plastics. We also give our perspective on the subfield of PLA block polymers, our outlook on the future, and our assessment of exciting developments yet to come.

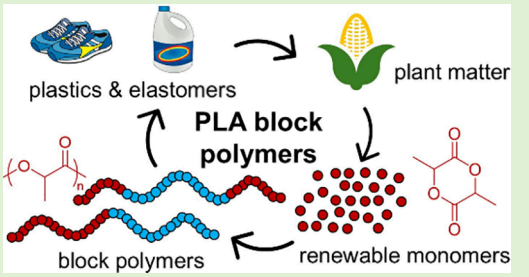

BACKGROUND AND MOTIVATION

Since its post-World War II beginnings, the modern polymer industry has established most of its markets in nonrenewable, single-use (often plastic) products. The single-use paradigm has been extremely profitable, as it inherently sustains demand while offering consumers lifestyle conveniences generally unmatched by other commodity materials.[1,2] By entrenching this mindset in our economy and everyday lives over the last half-century, society has created two crucial problems for plastics. The first is massive pollution. Roughly 80% of all plastics ever produced have been landfilled or mismanaged, disrupting terrestrial and aquatic ecosystems.[3,4] Beyond the destruction of habitats allocated for landfilling, ubiquitous macroscopic plastic waste and the derived microplastics pose novel toxicological threats to humans and other living organisms.[5−8] The second problem is our wholesale reliance on fossil feedstocks for these materials. Polymers have been a consistent driver of oil and gas demand growth for petrochemicals, and single-use plastic regulation is projected to hold the greatest influence over future demands on these nonrenewable resources.[9] Without system change, plastics' share of oil consumption will likely rise to ∼20% and its share of the carbon budget to ∼15% by 2050.[10] Along with shifts to renewable energy sources and environmental protection, a livable future depends on a circular plastics economy.

Such is the appeal of poly(lactide), or PLA. Lactide, the cyclic dimer of lactic acid, is renewably produced from bacterial fermentation of plant-based dextrose (D-glucose), most notably from corn.[11] The enantiomer of lactic acid enzymatically produced can be tuned by selection of the bacterial genus.[12] Hence, atactic, amorphous poly((±)-lactide) (sometimes labeled poly(D,L-lactide) or PDLLA); poly(*meso*-lactide); and the isotactic, semicrystalline poly((−)-lactide) (often labeled poly(L-lactide) or PLLA) and poly((+)-lactide) (often labeled poly(D-lactide) or PDLA) are readily accessible. (We note that the abbreviation "PLA" is often ambiguously used to refer to any or all the aforementioned tacticities; herein, we have taken care to identify PLA tacticity where appropriate.) Cargill's seminal 1993 patent for coupling lactide synthesis and its subsequent tin-catalyzed ring-opening transesterification polymerization (ROTEP) opened the door to scalable production of high-molar mass PLA, and with it, numerous market opportunities.[13] Due to PLA's broad compatibility with human tissues and tunable *in vivo* degradation, early research focused primarily on biomedical technology applications such as stents, cell scaffolding, drug delivery, resorbable sutures, and rigid surgical apparatuses, but has since expanded to a wide variety of consumer items.[14,15] PLA is amenable to typical polymer processing operations, including extrusion, injection and blow molding, thermoforming, and fiber spinning. PLA's high stiffness, strength, and transparency, similar to properties of poly(styrene) (PS), have placed most of its market presence in flexible and rigid packaging, fibers, and consumer goods.[16−18] The U.S. Food and Drug Administration permits the tin(II) 2-ethylhexanoate

Received: February 2, 2025
Revised: March 15, 2025
Accepted: March 18, 2025
Published: April 7, 2025

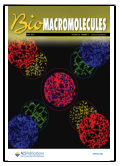

https://doi.org/10.1021/acs.biomac.5c00161
Biomacromolecules 2025, 26, 2761−2783

($Sn(oct)_2$) ROTEP catalyst at 1 wt % maximum in food-contacting resins[19] and in 2005 granted the first PLA food contact substance notification to NatureWorks LLC (a Cargill subsidiary),[20] allowing PLA produced using $Sn(oct)_2$ to enter the single-use-dominated food packaging market.[21] As an aliphatic polyester, PLA can be hydrolytically degraded in industrial composting conditions, enabling a closed-loop carbon cycle (CO_2 and H_2O generated in compost are taken up by plant feedstocks for PLA).[22] Amidst mounting concerns[23] about the ecotoxicological effects of micro- and nanoplastics, Holland Bioplastics recently commissioned HYDRA Marine Sciences for a meta-analysis of PLA degradation behavior. The authors posit that as long as moisture is available, even if outside of industrial composting conditions, PLA will continue to hydrolyze until the small molecule and oligomeric products are water-soluble, preventing the long-term buildup of micro- and nanoplastic particles.[24] The success of its applications has solidified PLA as the most widely produced synthetic, circular polymer. Its production capacity has exceeded forecasts and is expected to accelerate in the coming years (Figure 1),[25] promising ongoing contributions to the growing market for compostable plastics; under a comprehensive "system change scenario," compostables' share of the plastics market is expected to reach 9% by 2040.[26]

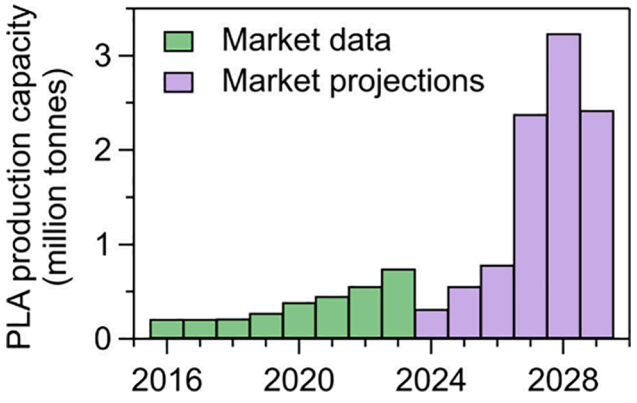

Figure 1. Realized and projected production capacities of PLA over time. Data were taken from European Bioplastics Market Updates from 2016 to 2024.[25]

Early investigations of PLA block polymers envisaged them as drug delivery vehicles, with co-blocks including poly(ε-caprolactone) (PCL)[27,28] and poly(ethylene oxide) (PEO).[29,30] We estimate that the largest PLA block in these early block polymer examples had a molar mass of ∼20 kg mol^{-1}, while the largest PLA species mentioned was a commercial ∼30 kg mol^{-1} PLA sold by Polysciences, Inc.[30] Cargill's commercial approach for controlled synthesis of high-molar mass PLA[31,32] offered polymer scientists designer, high molar mass PLA chains wherever there lay an exposed hydroxyl group, whether on a small molecule alcohol or a macroinitiator. The combination of synthetic control, renewable sourcing, biocompatibility, and biodegradability (under suitable conditions) led to an explosion of interest in PLA block polymers, with citations growing steadily before plateauing in the late 2010s (Figure S1). During that time, they have found use in, for example, microelectronics,[33,34] membranes and mesoporous materials,[35−38] drug delivery,[39,40] and thermoplastic elastomers.[41,42]

In this Perspective, we highlight the recent developments, successes, and current promise of PLA block polymers for a sustainable future (Figure 2). Here, we focus on materials that retain the PLA block at the end of preparation − that is, the PLA block is not purposefully etched or otherwise degraded (*e.g.*, as in nanoporous membrane applications). Additionally, we have deliberately excluded PLA−PEO block polymers from our scope, as there are already several excellent reviews chronicling these materials' rampant success in biotherapeutic applications.[40,43−45] The examples we have chosen are not exhaustive; they are representative of numerous modern and exciting advances in PLA block polymer science. We first overview key developments in PLA block polymer synthesis, along with several examples of PLA's utility in block polymer mesostructure discovery. Thereafter, we detail bulk materials-focused research on PLA block polymers, covering applications in adhesives, elastomers, and rigid plastics. Finally, we outline the opportunities for academic researchers to address remaining technological barriers to PLA's proliferation. By attuning to a broader range of value chain stakeholders' needs, polymer scientists can target more actionable material interventions to support the industry in keeping pace with the global sustainability commitments for the 21st century.

SYNTHESIS

The field of block polymer synthesis has seen enormous growth in the past half-century, and with those advancements comes the ability to tailor-make a vast array of macromolecules.[46] Perhaps the simplest case of PLA block polymer synthesis is the formation of aliphatic polyesters through the ROTEP of lactide with other lactones. However, judicious choice of catalyst, initiator, comonomer, and polymerization method(s) allows for almost any combination of polymeric segments to be synthetically joined in a block polymer. We highlight selected recent PLA block polymer advancements that enable the synthesis of unique structures that benefit from incorporation of various other segments.

Synthetic efforts that exploit the ability of PLA to form interesting crystalline phases have been recently advanced. It is well-known that isotactic PLLA or PDLA can crystallize into a 10_3 crystal structure.[47] Further, when blended together, PLLA and PDLA can form a stereocomplex (SC), a densely packed 3_1 crystal structure with an increased melting temperature (230 °C vs 180 °C), a higher crystal modulus (20 GPa vs 14 GPa), and more rapid crystallization kinetics compared to PLLA or PDLA alone.[48−51] However, when blending high molar mass chains, typically mixtures of homocrystallites and SC crystallites are observed due to slow polymer diffusion.[49] Covalently linking PLLA and PDLA into PLLA-*b*-PDLA block polymers, or stereoblock PLA, helps to surmount this kinetic barrier to stereocomplexation.[49,50] Facile synthesis of these stereoblock polymers *via* sequential polymerization of (−)-lactide and (+)-lactide[52−55] further advances the design of polymeric molecules for a diverse array of applications. Rosen *et al.* reported a highly active chloro-magnesium complex enabling controlled formation of stereoblocks (up to hexablocks) of PLA within minutes by way of a one-pot sequential addition method.[54] The resulting polymers' molar masses were narrowly distributed ($Đ \leq 1.07$), and they had melting temperatures of up to 215 °C.[54] Further work demonstrated the successful synthesis of PCL-*b*-PLLA-*b*-PDLA and PDLA-*b*-PLLA-*b*-PCL-*b*-PLLA-*b*-PDLA block polymers using the same chloro-magnesium complex.[55]

https://doi.org/10.1021/acs.biomac.5c00161
Biomacromolecules 2025, 26, 2761−2783

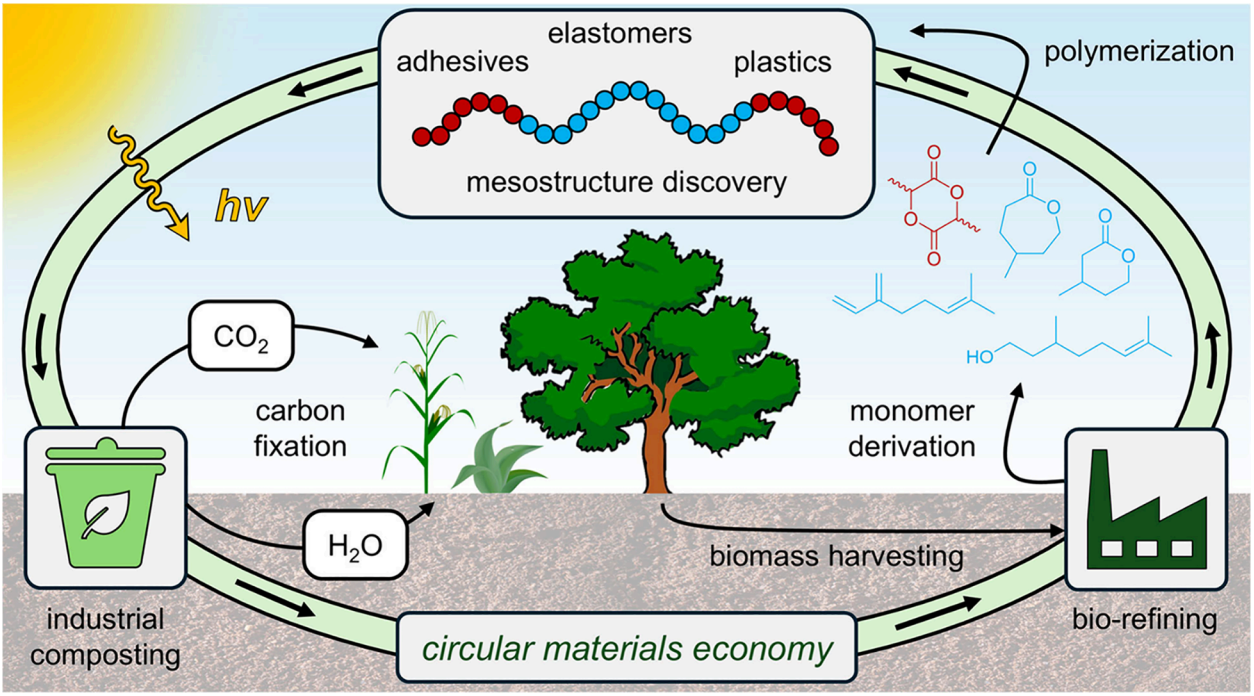

Figure 2. PLA block polymers can be bioderived and compostable, supporting a circular plastics economy.

Another way to synthesize stereoblock PLA is through the stereoselective polymerization of *rac*-lactide, which is an equimolar mixture of (−)-lactide and (+)-lactide.[56−61] Of these systems, organocatalytic (thio)ureas stand out as metal-free, highly active, and highly stereoselective.[56,59−61] These (thio)ureas often require a cocatalyst, and the following have been studied for this purpose: N-heterocylic carbenes,[59] phosphazene bases,[60] and cyclopropenimine.[61] These systems can reach high levels of stereoselectivity up to P_m = 0.93 (where P_m is the probability of meso dyads, or adjacent stereocenters with the same absolute configuration, typically quantified using ^{1}H NMR spectroscopy), with melting temperatures up to 189 °C.[59,60] Interest in SC PLA arises from the slow crystallization of the homochiral chains, which make it difficult to achieve high degrees of crystallinity using common industrial processing conditions such as injection molding, extrusion, and thermoforming.[62−64] The incorporation of SC PLA within block polymers improves the crystallization kinetics drastically, without the need for heterogeneous nucleating agents, such as talc or clay.[64] Combined with the higher crystal modulus of SC PLA, this is a promising way to improve the readiness of PLA block polymers for common industrial processing methods.

PLA block polymers have historically been synthesized through anionic[27,65−67] or cationic[68,69] polymerization of comonomer(s) followed by ROTEP of lactide from the hydroxyl-terminated end(s). Orthogonal initiation offers another method of synthesizing block polymers with chemically dissimilar monomers and different polymerization methods. Initiator molecules with distinct initiation sites have been used to create block polymers combining ROTEP of lactide with, for example, atom transfer radical polymerization (ATRP), reversible addition−fragmentation chain transfer polymerization (RAFT), ring-opening metathesis polymerization (ROMP), and nitroxide mediated polymerization (NMP) (Figure 3). Albanese *et al.* describe the

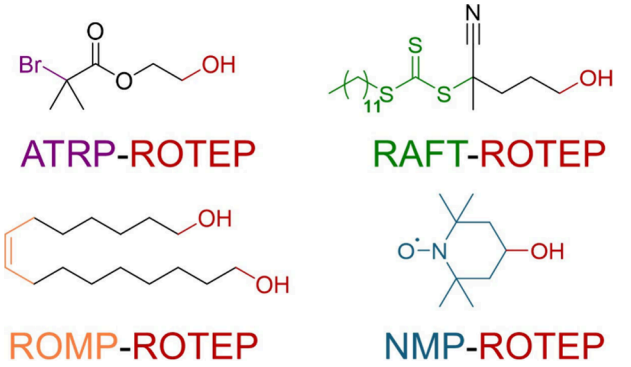

Figure 3. Example orthogonal initiators that have been explored to combine distinct polymerization methods to create a diverse array of PLA block polymers, including ATRP-ROTEP,[70] RAFT-ROTEP,[71] ROMP-ROTEP,[38] and NMP-ROTEP.[73]

synthesis of PLA-*b*-poly(γ-methyl-ε-caprolactone)-*b*-PS ABC triblock polymers with 2-hydroxyethyl-2-bromoisobutyrate, which can serve as the initiator for ROTEP followed by ATRP.[70] Importantly, the ATRP chain end needs to be stable under ROTEP conditions, allowing for the ROTEP of γ-methyl-ε-caprolactone (γMCL) then lactide which is followed by the polymerization of styrene under ATRP conditions.[70] Yildirim *et al.* introduced sequential ROTEP-RAFT polymerization using a hydroxyl-containing chain transfer agent allowing for the ROTEP of lactide followed immediately by RAFT of 2-hydroxyethyl acrylate without any intermediate purification or deprotection steps.[71] The combination of ROTEP and ROMP has been accomplished by using a dihydroxy alkene-containing initiator *via* either a ROTEP-first procedure,[72] or ROMP-first method using poly(cyclooctene).[38] Another example is the combination of NMP and ROTEP in the synthesis of PS−PLA block polymers using a hydroxyl-functionalized TEMPO molecule as the initiator.[73] Finally, we highlight the work of Bolton and Rzayev

https://doi.org/10.1021/acs.biomac.5c00161
Biomacromolecules 2025, 26, 2761−2783

who describe the three-step process of synthesizing PS-*b*-poly(methyl methacrylate)-*b*-PLA triblock bottlebrush polymers *via* sequential ATRP, RAFT, and ROTEP, through the use of a macroinitiator with orthogonal, albeit protected, initiation sites.[74] The combination of ROTEP with alternative controlled polymerization methods showcases the variety of well-defined block polymers that can be synthesized with PLA segments.

In addition to block polymerization *via* sequential monomer addition as described above, there have also been efforts to explore the synthesis of PLA block polymers using one-pot, mixed monomer feedstocks of lactide and comonomer(s). The ability to combine ROTEP of lactide with alternative polymerization methods *via* switchable catalysis is a powerful platform to synthesize block and multiblock polymers from mixed monomer feedstocks. In 2014, the Williams group pioneered such switchable catalysis, which describes the process of creating block polymers through a catalyst system that can 'switch' between distinct polymerization mechanisms, primarily ring-opening copolymerization (ROCOP) and ROTEP (Figure 4).[75,76] Since then, there have been many

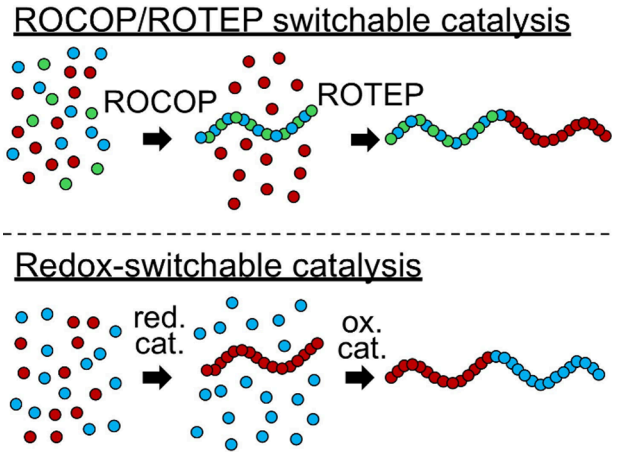

Figure 4. Switchable catalysis methods used to polymerize PLA block polymers.

investigations into switchable catalysis as a means to synthesize PLA block polymers. In one of the first examples, Stößer *et al.* demonstrated the block copolymerization of propene oxide/phthalic anhydride and lactide using an aluminum salphen catalyst.[77] They created multiblock polymers through sequential addition of monomer mixtures, where after each addition, ROTEP of lactide occurred only after high conversion (>95%) of phthalic anhydride.[77] Further, they found that the monomer insertion of the ROCOP step is zero order, while the lactide insertion is first order, explaining why ROCOP proceeds first. While many switchable catalysis methods rely on metal catalysts,[76] Geng *et al.* developed a switchable organocatalyst, a boron-containing thiourea, to catalyze the sequential polymerization of propene oxide/carbonyl sulfide and lactide.[56] Only ROCOP of propene oxide and carbonyl sulfide was found to occur in the mixture of all monomers, while only ROTEP of lactide was found to occur in the absence of carbonyl sulfide.[56] Around the same time that the Williams group introduced switchable catalysis between ROCOP and ROTEP, the Diaconescu group explored block polymerization of lactide and ϵ-caprolactone using redox-switchable titanium and zirconium catalysts.[78] They found that in the presence of both lactide and ϵ-caprolactone, a titanium-thiolfan complex would almost exclusively polymerize lactide to modest conversion (58%); whereupon the addition of an oxidant, the titanium catalyst would then polymerize almost exclusively ϵ-caprolactone, again to modest conversion (18%). Byers and co-workers also applied the idea of switchable catalysis of lactide to redox-switchable iron catalysts.[79−81] They demonstrated that given mixtures of lactide and cyclohexene oxide (CHO), block polymers of the type AB and BA can be synthesized using an *in situ* redox switch, with block order dictated by the oxidation state of the iron catalyst.[80] This same catalyst can be used to create triblock polymers PLLA-*b*-poly(tetrahydrofuran (THF)-*co*-CHO)-*b*-PLLA by switching the redox catalyst between Fe(II) and Fe(III) oxidation states.[79]

Polymer architecture plays an important role in polymer properties, and the ability to create PLA block polymers with well-defined architectures using ROTEP has been the subject of many investigations. The simplest linear examples of diblock and triblock structures can be synthesized *via* mono- or difunctional small molecule initiators. Linking these di- or triblocks together with difunctional chain extenders allows for the creation of linear multiblocks.[72,77,82,83] Accessing star block architectures is simply a matter of increasing the number of hydroxyl groups on a given initiator.[53,84−86] More complex block architectures, such as miktoarm stars and H-shaped polymers (Figure 5), require more synthetic manipulation but uncover unique polymer properties; here, we highlight some recent innovative approaches.

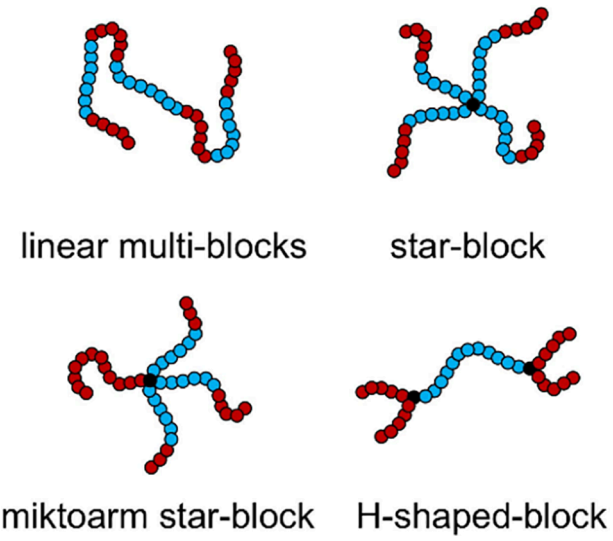

Figure 5. Representation of some of the various architectures explored in PLA block polymers.

A miktoarm star is characterized as a star architecture with one or more chemically distinct arms, which can often pose a synthetic challenge.[87] An approach taken by Blankenship *et al.* utilized a method termed μSTAR,[88] which is a type of grafting-through mechanism that allowed the creation of miktoarm stars with easily varied numbers of arms.[89] The synthesized polymers consisted of an average of three, six, or nine PγMCL-*b*-PLLA arms attached to one PLLA arm. The authors found that increasing the number of arms improved the strength, toughness, and recovery of the resultant thermoplastic elastomers. In contrast to the star architecture, which has

https://doi.org/10.1021/acs.biomac.5c00161
Biomacromolecules 2025, 26, 2761−2783

Table 1. Compiled Values of $\chi_{eff}(T)$ Fitting Parameters for PLA and the Listed Co-Blocks[a]

co-block, abbreviation	α (K)	β	determination method	V_{ref} (Å^3)	ref.
poly(ethylene oxide), PEO *OR* poly(ethylene glycol), PEG	not given	[−0.161, −0.048], dependent on PEO end-group	melting point depression[b]	N/A	97
poly(methyl methacrylate), PMMA	−2	0.01	RPA fits, binary interaction model[b]	118	98
poly(allyl glycidyl ether), PAGE	68.8 ± 9.4	−0.212 ± 0.030	RPA fit[b]	not given	99
poly(caprolactone), PCL	28.7 ± 2.0	−0.03 ± 0.005	rheology[b]	118	100
poly(γ-methyl-ε-caprolactone), PγMCL	51.6 ± 2.1	−0.07 ± 0.01	rheology	118	101
poly(6-methyl-ε-caprolactone), P6MCL	61.2	−0.1	rheology	118	102
poly(ε-decalactone), PDL	69.1 ± 9.2	−0.072 ± 0.026	rheology	118	103
poly(styrene), PS	98.1	−0.112	rheology, SSL spacings[b]	185	35
poly(butadiene), PB (36 mol % 1,4 units, 64 mol % 1,2 units)	161.6	−0.223	rheology	118	104
poly(1,4-isoprene), PI	230 ± 60	−0.38 ± 0.14	rheology	110	105
poly(cyclohexylethylene), PCHE	222 ± 15	−0.29 ± 0.03	rheology	118	106
poly(trimethylsilylstyrene), PTMSS	51.3	0.29	RPA fit	118	107
poly(ethylene), PE	150.8	not given	solubility parameters[b]	not given	108
poly(11-aminoundecanoic acid), polyamide 11, PA11	426 ± 4.81	−0.90 ± 0.01	rheology	118	82
poly(menthide), PM	364	−0.50	SSL spacings	arb.	109
poly(ethylene-*alt*-propylene), PEP (90−93 mol % 1,4 units)	445	−0.64	rheology	174	110
poly(dimethylsiloxane), PDMS	360	0.21	SSL spacings	118	111

[a]The values are ordered low-to-high when evaluated at T = 298 K. Co-block abbreviations are used throughout the remainder of the Perspective. [b]χ determination methods are elaborated on in the Supporting Information.

only a single branch point, the H-shaped or dumbbell polymer consists of two branch points and is of interest due to its unique rheological properties. However, they can be difficult to synthesize in a well-defined manner.[90,91] Recent advances have shown that end-functionalizing a telechelic linear polymer chain with two or more hydroxyl groups enables subsequent ROTEP of lactide.[91−93] While these are just a few examples of architecturally interesting PLA block polymers, it is important to note that varying architecture can have dramatic effects on both the self-assembly behavior of the block polymers as well as the ultimate mechanical properties. The ability to create architecturally diverse polymers is a key aspect in the development of designer macromolecules.

PLA BLOCK POLYMERS AS MESOSTRUCTURE DISCOVERY PLATFORMS

Block polymers' appealing hybrid properties arise directly from their nanocomposite-like mesostructures. Moreover, the study of block polymer mesostructure has blossomed into a rich subfield.[46] Investigations of this type typically aim to create new morphologies through chemical or architectural manipulations; expand design spaces or processing methods for morphologies useful for specific applications; or fabricate devices evaluating such new compounds in these applications. Especially over the last two decades, PLA block polymers have offered a particularly useful platform for mesostructure studies, an important aspect of their scientific merit to which we have devoted this section.

As synthetic efforts expand PLA's co-block scope, each new block introduced interacts differently with PLA by virtue of its distinct repeat unit structure, which presents opportunities for research on block polymer mesostructures. The interaction parameter, χ, encodes the strength of block interactions: a higher χ value signals a more unfavorable interaction. For convenience, most experimentalists use an operational definition, χ_{eff}, which encompasses the excess free energy of mixing for co-block pairs:[46,94]

$$\chi_{eff,A-B}(T) \equiv \frac{(\Delta G)^{ex}_{mix}}{f_A f_B k_B T} = \frac{(\Delta H)^{ex}_{mix} - T(\Delta S)^{ex}_{mix}}{f_A f_B k_B T} = \frac{\alpha}{T} + \beta \quad (1)$$

where f_A and f_B are the volume fractions for blocks A and B, and α and β respectively encapsulate the enthalpic and entropic contributions to χ. $\chi_{eff}(T)$ is estimated by fitting models to data obtained from experiments that manifest the excess properties of block mixing. Multiplying the $\chi_{eff}(T)$ for a block polymer's constituent blocks by its overall volume-referenced degree of polymerization (N) produces its "segregation strength," χN. Self-consistent field theory (SCFT) can then be used to generate block polymer morphology maps, which describe equilibrium domain morphologies resulting from block−block segregation as a function of f and χN, and predict order−disorder transition temperatures (T_{ODT}), above which block mixing occurs.[95,96] Table 1 lists $\chi_{eff}(T)$ functions for PLA-(co-block) pairs collected from the literature. We also note the Hildebrand solubility parameter (δ) for PLA in the Supporting Information, which allows for estimation of χ for many other co-blocks whose δ values are known. However, these quantities are measured indirectly or estimated and generally carry greater error.

PLA offers unique utility for block polymer ordered structure discovery. Controlled anionic polymerization of hydrocarbon monomers such as styrene, butadiene, and isoprene can easily be terminated with ethylene oxide to create telechelic hydroxyl end-groups for subsequent chain extension with lactide.[66] PLA's rather polar repeat unit interacts unfavorably (*i.e.*, high χ) with these anionically

https://doi.org/10.1021/acs.biomac.5c00161
Biomacromolecules 2025, 26, 2761−2783

polymerized blocks and their hydrogenated derivatives. A large χ provides a large χN even at low-to-moderate molar masses (N), which encourages rapid self-assembly of equilibrium morphologies. In contrast, a lower χ would require much larger blocks for an equivalent χN, which tends to incur kinetic barriers to ordering due to entanglements slowing chain diffusion. Hence, PLA offers a broad range of co-blocks for extremely well-defined, rapidly self-assembling block polymers. Here, we highlight key examples of this useful strategy.

In their simplest forms, block polymer segregation theories assume monodisperse chains, while even the most controlled polymerization schemes produce chains with molar mass dispersity. Hence, controlled manipulation of block dispersity offers valuable insight for theoretical refinements. Lynd and Hillmyer accomplished this with a series of PEP-*b*-PLA diblock polymers in which they exploited the reversibility of lactide ROTEP to tune the PLA block's dispersity ($Đ_{PLA}$). By increasing the reaction duration after the equilibrium conversion was achieved, they allowed more chain length scrambling through random monomer addition and removal at active chain ends, increasing $Đ_{PLA}$.[112] In symmetric ($f_A \approx f_B \approx 0.5$) diblocks, the lamellar domain spacings increased with $Đ_{PLA}$ compared to the monodisperse prediction from the strong segregation limit (SSL). The most strongly segregated diblocks experienced less domain swelling, though their domain spacings were more sensitive to $Đ_{PLA}$. Additionally, increasing $Đ_{PLA}$ at constant f_{PLA} changed the ordered morphology for more weakly segregated diblocks. When PLA was the minority domain, increasing $Đ_{PLA}$ increased the curvature toward PLA (LAM → GYR → HEX), while the opposite was true (GYR → LAM, HEX → GYR) when PLA was the majority domain. These results supported contemporary theory[113] that larger chains, which are more abundant in polydisperse blocks, can stretch to fill space inside curvature with less entropic penalty than short ones, encouraging spontaneous curvature toward more polydisperse blocks. Furthermore, they observed a composition-dependent shift in $(\chi N)_{ODT}$ with increasing $Đ_{PLA}$: $(\chi N)_{ODT}$ decreased at low f_{PLA}, signifying stabilization of ordered morphologies, but increased at high f_{PLA}, indicating destabilization, the latter in contradiction with SCFT predictions. Schmitt and Mahanthappa later investigated the effects of "B" midblock dispersity in PLA-*b*-poly(1,4-butadiene)-*b*-PLA (LBL) triblock polymers. In a compositionally symmetric LBL library (f_B = 0.49−0.54), the tendency for curvature toward the polydisperse B blocks ($Đ_B$ = 1.7−1.9) shifted the LAM phase window to higher f_B than for more monodisperse B blocks ($Đ_B$ < 1.1).[114] Shortly thereafter, they explored a wider compositional range (f_B = 0.26−0.95), finding that in addition to shifting ordered phase windows to higher f_B, increasing $Đ_B$ globally increased the segregation strength required for microphase separation ($\chi N \geq 27$) relative to the monodisperse case ($\chi N \geq 17.9$), mirroring Lynd and Hillmyer's high-f_{PLA} result.[115,116] This was ascribed to enhanced concentration fluctuations occurring at low N further strengthened by the compositional dispersity entailed by high $Đ_B$, which destabilized ordered morphologies.

Sparsely branched architectures offer other means of controlling domain interfacial curvature. Ma *et al.* synthesized PDMS−PLA block oligomers while modulating the architecture from 3(AB) (diblock arm star) to 3AB (linear-branched) to $3(AB_1)B_2$ (homodiblock miktoarm star), with A = PDMS and B = PLA and f_{PLA} ranging from 0.41 to 0.57 (Figure 6).[117] Consistent with SCFT predictions,[118] the 3(AB) had similar

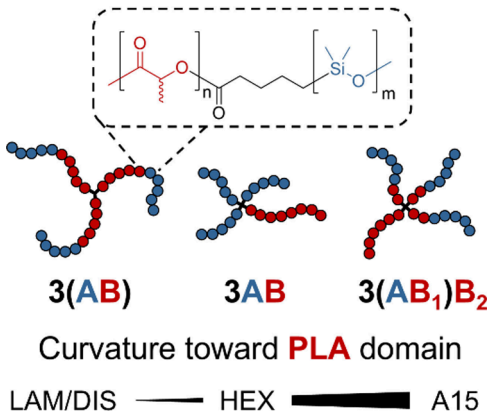

Figure 6. Changing the proximity between the branching node and block junction modulates domain interfacial curvature in PDMS-*b*-PLA block oligomers.[117]

phase behavior to that predicted for the AB diblock arms − namely, all microphase separated samples adopted a LAM morphology. With the block junctions located at the branching point in linear-branched 3AB, interfaces curved away from the PDMS chains to reduce chain crowding, remarkably enabling PLA cylinders to persist up to f_{PLA} = 0.55. In $3(AB_1)B_2$, the small spacer between the block junctions and branching point relieved packing frustration in the discrete PLA domain. As a result, $3(AB_1)B_2$ assembled a higher-curvature, sphere-packing Frank-Kasper A15 morphology with f_{PLA} = 0.4, and its HEX stability limit was further deflected to f_{PLA} > 0.57. These results validated more recent SCFT investigations into miktoarm star polymers.[119] Meier-Merziger *et al.*'s "super-H-shaped" $(PLLA)_3$-*b*-PI-*b*-$(PLLA)_3$ block polymers showed similar effects with f_{PLLA} ranging from 0.16 to 0.28. Despite the conformational asymmetry between PLLA and PI,[93,120] which would tend to shift ordered phase boundaries to higher f_{PLLA},[96] the branching-induced resistance to curvature in the PLLA domain produced HEX/LAM coexistences for most samples and even solely LAM for f_{PLLA} = 0.28. In a similar vein, with a more conformationally symmetric block pairing, Pitet *et al.* achieved a LAM morphology with f_{PLA} = 0.09 in $(PLA)_2$-*b*-poly(cyclooctene)-*b*-$(PLA)_2$.[121]

Much more densely branched PLA-containing bottlebrush polymers have yielded surprising morphological discoveries through experimentation with frustration, meaning the relationship between blocks' topological connections and their chemical compatibility. Bolton and Rzayev's PS−PMMA−PLA triblock bottlebrush polymers separated the incompatible PS and PLA (χ_{PS-PLA} = 0.23 at 25 °C) along an acrylate backbone with a "mutually agreeable" PMMA brush-block ($\chi_{PS-PMMA}$ = 0.032, $\chi_{PMMA-PLA} = 3.3 \times 10^{-3}$ at 25 °C).[74] Despite sufficient χN for predicted separation, the PS and PMMA brush-blocks mixed and separated from PLA, producing an unexpected lamellar morphology. Cui *et al.* more recently synthesized similarly nonfrustrated[122] ABC triblock bottlebrushes ($\chi_{AC} > \chi_{AB} \approx \chi_{BC}$) featuring a PEP−PS-PLA brush-block sequence.[123] They observed a novel cylinders-in-undulating-lamellae (CUL) morphology, with PLA cylinders located between undulating PEP lamellae in a PS matrix. CUL was thermodynamically stable within a surprisingly wide PS-rich compositional space. The *Fddd* network phase was absent from the morphology portrait compared to linear triblock analogues, while the core−shell

https://doi.org/10.1021/acs.biomac.5c00161
Biomacromolecules 2025, 26, 2761−2783

GYR phase remained, which the authors attributed to a reduction in effective PEP−PLA contact caused by the stiffness of the triblock bottlebrush backbone.

The accessibility of optically enriched lactide feedstocks makes the isotactic PLAs useful for studying block polymer crystallization. Zhou *et al.* created a series of PLLA-*b*-poly(butylene terephthalate)-*b*-PLLA triblock polymers with a 1.6 kg mol^{-1} midblock and PLLA weight fraction (w_{PLLA}) ranging from 0.81 to ∼0.99.[124] Increasing w_{PLLA} suppressed midblock crystallization, while the PLLA crystallization temperature and overall crystallization rate peaked when the PLLA arm molar mass was ∼20 kg mol^{-1}, possibly reflecting an interplay of insufficient thermodynamic drive for crystallization in the short PLLA blocks and entanglements in the longer PLLA blocks slowing crystallization kinetics. As homopolymers, PLLA and PDLA form crystal lamellae helically twisted along the lamellar plane (perpendicularly to chain axis), with chain stereochemistry controlling the twisting direction.[125] Maillard and Prud'homme ascribed this effect to the homochiral backbone creating a stress imbalance across the lamellar fold surfaces.[125] In their study of PS-*b*-PLLA diblocks (f_{PLLA} = 0.65) with polarized optical microscopy, Chao *et al.* observed banded spherulites, in which periodic birefringence extinctions appear along the spherulites' radial axes, diagnostic of the same lamellar twisting phenomenon.[126] The twisting occurred over a wider range of crystallization temperatures than for PLLA homopolymer, and when measurable for both species, the helical pitch length was considerably smaller for PS-*b*-PLLA. The authors reasoned that the microphase separated PS coils enhanced the homopolymer's lamellar stress imbalance, encouraging tighter lamellar helices.

After the discovery of helical domain morphologies in PS-*b*-poly[isocyano-di(amino acid)]diblocks,[127] the comparative synthetic ease of installing PLLA or PDLA co-blocks propelled PLA block polymers to the forefront of chiral phase discovery. Huang and co-workers first documented helical PLLA domains with 2-fold symmetry, the so-called "H*" phase, in PS-*b*-PLLA diblocks with f_{PLLA} = 0.35.[128] Later, they expanded the phase window, observing H* from 0.32 ≤ f_{PLLA} ≤ 0.39, as well as its instability at long annealing times.[129] They measured a higher persistence length for PLLA than for atactic PLA, suggesting that PLLA's helical steric hindrance increased its chain rigidity. From this result, they speculated that the PLLA conformations near the interface that would minimize self-hindrance encouraged relative twisting among adjacent chains, leading to H*. Circular dichroism and fluorescence spectroscopies on PS-*b*-perylene-*b*-PLLA in the H* phase later directly evinced the twisting at the block junction and resultant domain layer shifting necessary to produce H*.[130] More recently, by comparing ABC triblocks PS-*b*-PEO-*b*-PLLA (B and C miscible) and PS-*b*-poly(4-vinylpyridine)-*b*-PLLA (B and C immiscible), Yuan et al. found that the chirality effect could transfer from PLA to PEO with a short PEO midblock to create the H* phase with chain-mixed domains.[131] Additionally, with f_{PLA} ≈ 0.5, PI-*b*-PS-*b*-PLLA and PI-*b*-PS-*b*-PDLA triblocks formed a novel single/double GYR coexistence in which the PLA single gyroid domain's chirality was controlled by the choice of PLLA or PDLA.[132] Together, the ongoing study of isotactic PLA-containing block polymers' crystallization and domain helicity has solidified the understanding of chain-to-superstructure chirality information transfer.

PLA BLOCK POLYMERS IN THE MATERIAL ECONOMY

This section details the mechanical properties accessible by PLA block polymers in order of increasing PLA volume fraction (Figure 7). PLA block polymers that have a minority

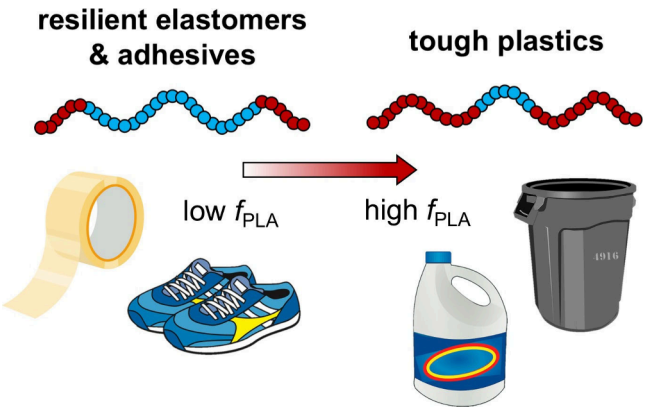

Figure 7. Schematic representation of block polymers with low and high f_{PLA} and potential applications.

volume fraction of PLA (f_{PLA} ≤ 0.50) can function as pressure-sensitive adhesives (PSAs) and thermoplastic elastomers (TPEs). These applications typically require a rubbery (*i.e.*, low T_g) midblock that serves as a matrix within which spherical or cylindrical PLA domains act as physical cross-links. As we move toward block polymers with a majority fraction PLA (f_{PLA} ≥ 0.50), we begin to access rigid plastic behavior such as that of PS, poly(ethylene terephthalate) (PET), and high-density poly(ethylene) (HDPE). While less studied than their elastomeric counterparts, these materials demonstrate some of the unique benefits of PLA block polymers within plastics.

Pressure-Sensitive Adhesives. PSAs enable the products that consumers stick to surfaces. Stickers, sticky notes, stamps, bandages, tapes, labels, Command products (3M), and a host of other consumer goods bond to a wide range of substrates solely under pressure, without relying on solvent evaporation, temperature changes, or chemical reactions.[133] PSAs exhibit "permanent tackiness," wetting substrates on short time scales and usually with mild pressure. Block polymer-tackifier blends make up one class of PSAs. The earliest materials featured PS-lean, PS-*b*-PI-*b*-PS (SIS) or PS-*b*-PB-*b*-PS (SBS) triblock polymers in which glassy, microphase separated PS domains acted as physical cross-links for the rubbery, matrix-forming midblock.[134] Tackifiers, often low molar mass resins, dilute midblock entanglements to increase the effective molar mass between entanglements (M_e) and enhance tackiness. The segregated SIS/SBS nanostructure endows them with superior creep resistance to other, one-phase commercial PSAs, including rubber-tackifier composites and acrylate copolymer-tackifier blends.[133]

PLA has found use as a sustainable replacement for the PS block in PSAs, as it is also glassy at room temperature and has similar stiffness characteristics. Shin *et al.* first reported a renewable PSA including PLA-*b*-PM-*b*-PLA triblocks and a Sylvalite rosin ester tackifier with best adhesive properties (60 wt % triblock) competitive with duct, paper, and electrical tapes.[135] The hydrolytic degradability of the triblock polyester also offered a possible solution for the accumulation of residual adhesives or "stickies" in the pulp and paper recycling

https://doi.org/10.1021/acs.biomac.5c00161
Biomacromolecules 2025, 26, 2761−2783

industry.[136] Lee *et al.* later expanded the midblock scope, combining as low as 35 wt % PLLA-*b*-PDL-*b*-PLLA triblocks with rosin ester and epoxidized soybean oil plasticizer to achieve peel and shear resistance properties between Scotch tape and duct tape.[137] The limits of tackifier miscibility were clarified for a PLA-*b*-poly(*β*-methyl-*δ*-valerolactone)-*b*-PLA triblock, which could solubilize only up to 50 wt % Sylvalite before macrophase separating.[138] Linear viscoelastic analysis, cross-referenced with Chang's window analysis,[139] identified these materials as competitive candidates for general use or easily removable PSAs. Additionally, this study showed that controlled rheological experiments could rationalize trends observed in standard PSA tests: uniaxial extension for peel adhesion, small-angle oscillatory shear for loop tack, and shear creep for shear resistance. Xu *et al.* recently described a library of PLLA-*b*-poly(alkyl-*δ*-lactone)-*b*-PLLA triblocks that could achieve commercially competitive peel strength without tackifier.[140] The lack of tackifier enabled chemically recyclable PSAs through staged reactive distillations, which sequentially recovered PLLA as ethyl lactate and pure midblock lactone monomer, respectively.

Kim *et al.* introduced cashew shells as another renewable feedstock for PLA-containing PSAs.[141] They used cardanol, a downstream product of the cashew industry, to produce poly(pentadecylcaprolactone)s (PPDCL) as midblocks, desirable for their large M_e, which in principle offers greater intrinsic tackiness. With high tackifier loadings (60−80 wt %), these PLA-*b*-PPDCL-*b*-PLA ("LPL") PSAs displayed excellent properties, surpassing duct tape in peel and loop tack force and matching office tape in shear resistance (Figure 8). One

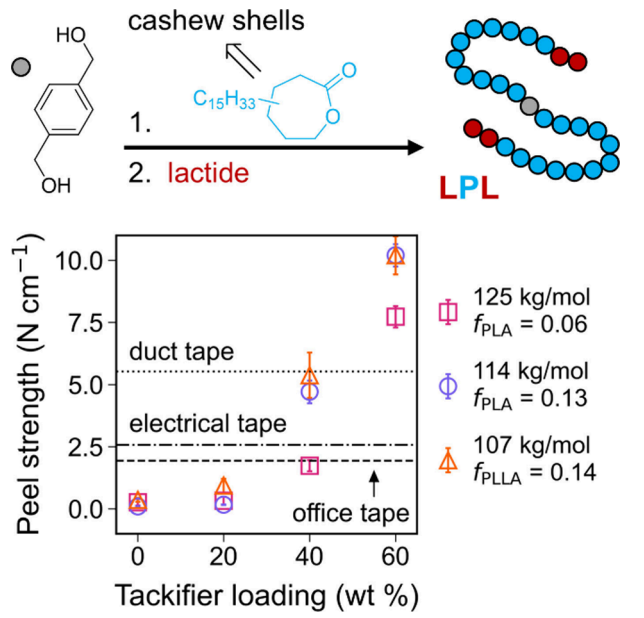

Figure 8. LPL triblock synthesis scheme and adhesive properties.[141]

LPL with semicrystalline PLLA end-blocks resisted shear failure for over 6000 min, whereas similar triblocks with atactic PLA end-blocks failed earlier, highlighting the importance of hard domain crystallinity for shear resistance. Interestingly, the crystallinity in the long PPDCL alkyl chains enabled temperature-switchable properties. Briefly heating the substrate to 38 °C to melt PPDCL side-chains enabled better adhesion, a promising result for body-temperature activated adhesives, while cooling before debonding promoted adhesive failure by crystallizing the side-chains. Advantageously for waste management, the LPL triblocks were also readily degraded in acidic THF.

In a similar vein, Liang *et al.* prepared PSAs by blending renewable tackifier with low-f_{PLLA} PLLA-*b*-P*γ*MCL-*b*-PLLA triblock polymers.[142] Solvent casting these materials led to weakly microphase separated PLLA domains, which produced limited peel and loop tack forces. Annealing the samples in two stages − one stage at 170 °C to form better defined PLLA domains and a second at 100 °C to crystallize the PLLA − increased the peel strength 3-fold, maximized shear resistance, encouraged desirable adhesive failure, and bolstered the adhesive characteristics over long aging periods. The triblock was fully degraded in aqueous base over 15−25 days, offering a sustainable end-of-life pathway.

Thermoplastic Elastomers. TPEs combine the processability of thermoplastics and the rubbery elasticity of crosslinked elastomers at room temperature. These materials are commonly ABA triblock polymers featuring hard A end-blocks (high T_g or T_m) flanking a rubbery B midblock (low T_g).[143] The SIS and SBS triblocks described in the previous section were the original commercially successful variants, and were introduced to the commercial market as components of leisure footwear under the name Kraton by the Shell chemical company in the 1960s.[2] To this day, styrenic block polymers such as SIS and SBS remain the most produced TPEs according to a report by Grand View Research.[144] These styrenic materials are desirable for their high tensile strength (>20 MPa), high extensibility (>1000%), transparency, and robust elastic recovery behavior. Many researchers have taken advantage of the material similarities between PS and PLA to develop a new generation of TPEs with PLA end-blocks, starting in the late 1990s. These early TPEs featured PDMS,[145] poly(isobutylene),[69] and PI[67] midblocks. Over the past three decades, these PLA-based TPEs have progressed immensely. As demonstrated by the works highlighted in this section, recent PLA-based materials compete with these incumbent TPEs in terms of tensile strength and extensibility (Figure 9), while maintaining elastic-recovery behavior and transparency. Further, semicrystalline PLLA-based TPEs exhibit a higher upper service temperature than styrenic TPEs ($T_{g,PS} \approx 100$ °C,

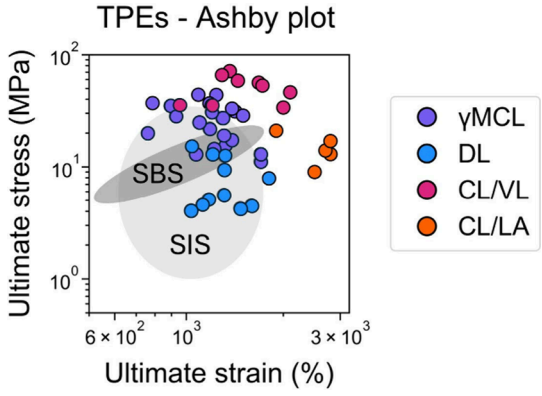

Figure 9. Compiled tensile properties of TPEs with PLA-based hard segments and various midblocks compared to commercial SIS and SBS, adapted from a report by Gregory *et al.*[146] CL/LA = poly(*ε*-caprolactone-co-(±-lactide))

https://doi.org/10.1021/acs.biomac.5c00161
Biomacromolecules 2025, 26, 2761−2783

$T_{m,PLLA}$ ≈ 160 °C), broadening the usage temperature range for this class of materials.

Substituted caprolactones have been extensively explored as the rubbery midblock within PLA-based aliphatic polyesters. PM,[42,109] P6MCL,[102] PDL[86,103] and PγMCL[53,70,84,89,101,147] have each been explored as a rubbery counterpart to PLA within TPEs, with the latter commanding much of the focus to date (Figure 10). The desirable traits of PγMCL include its low

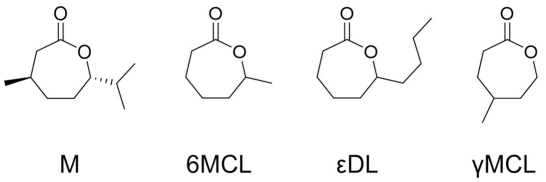

Figure 10. Selected substituted caprolactones used as the rubbery midblock within PLA block polymers as TPEs. Monomer abbreviations can be found in Table 1.

entanglement molar mass (M_e = 2.9 kg mol^{-1}),[101] its degradability,[148,149] and low cytotoxicity.[150] Further, its monomer γMCL can be sourced from *para*-cresol,[53] which in turn can be derived from renewable resources. In 2017, Watts *et al.* published important initial work exploring PγMCL within PLA-block polyesters, inspiring a host of related PLA-*b*-PγMCL research in the time since, much of it probing the mechanical and morphological effects of architecture.[101] Liffland and Hillmyer studied the impact of the star architecture within PLLA-*b*-PγMCL block polymers. In this system, the authors found that increasing the number of arms from two (linear) to four or six arms while keeping the overall molar mass the same resulted in higher ultimate tensile strengths (31−33 MPa) and Young's moduli (4−5 MPa), with only slight decreases in the elongation at break (∼1400%).[84] Blankenship *et al.* expanded the architectural portfolio with a library of PLLA-(PγMCL-*b*-PLLA)$_n$ A$_1$(BA$_2$)$_n$-type miktoarm stars. Adopting a miktoarm star architecture deflects block polymer phase boundaries, allowing for a higher f_{PLLA} while maintaining discrete spherical or cylindrical domains, which are necessary for ideal TPE performance (*i.e.*, no plastic deformation). Their PLLA-(PγMCL-PLLA)$_n$ stars resisted plastic deformation with f_{PLLA} up to 0.52, which would otherwise only be expected from network or lamellar morphologies.[89] Another architectural variant of PLLA-*b*-PγMCL based materials explored by Fournier *et al.* utilized a graft architecture, with a PγMCL backbone and PLLA arms. They achieved remarkably tunable properties by varying the grafting density, graft length, and w_{PLLA}, with a high grafting density proving to be most crucial attribute for robust mechanical properties.[147]

One of the most important properties of TPEs is their elastic recovery behavior, which can be measured through hysteresis testing and stress relaxation analyses. These experiments emulate how a material would respond to external stress during typical usage. In hysteresis testing, a material's nonrecoverable strain, or creep, after repeated load is measured, while stress relaxation analyses measure a material's time-dependent stress response to an applied strain. TPE applications require minimal creep and stress relaxation. Linear TPEs can perform well in both categories, but there are ways to reduce both the strain hysteresis and stress relaxation. One involves using semicrystalline PLLA as the end-block instead of amorphous PLA.[42,101] Building off this idea, Liffland *et al.* installed stereoblock PLA (that is, PLLA-*b*-PDLA) as the end-blocks within four-arm star polymers with a PγMCL midblock. Compared to the stars with only PLLA as the end-blocks, the stars with PLLA-*b*-PDLA end-blocks exhibited improved elastic recovery and retention of elasticity as measured by hysteresis and stress relaxation analyses respectively, while maintaining ultimate tensile strengths and elongations.[151] In another attempt to improve the elastic recovery of the PLLA-*b*-PγMCL based materials, Albanese *et al.* synthesized PLLA-*b*-PγMCL-*b*-PS ABC triblock polymers. Whereas the ABA architecture permits mechanically weak loops with both hard end-blocks anchored in the same domain, this ABC architecture forces the PγMCL to bridge separate hard domains due to the immiscibility of PLLA and PS (Figure 11). In hysteresis testing, the authors reported up to 98% recovery over 10 cycles for the ABC system, compared to 90 and 95% for the ABA and CBC type materials.[70]

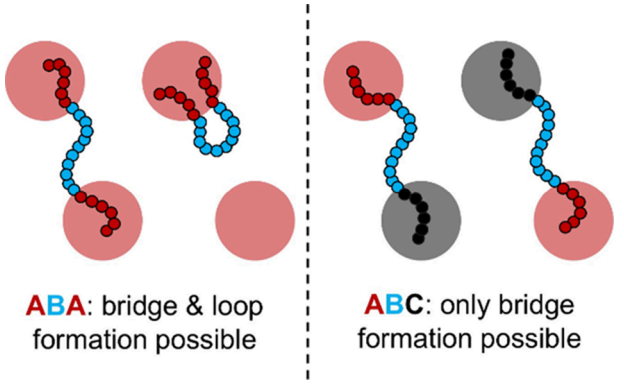

Figure 11. Possible polymer chain configuration of ABA- (left) and ABC- (right) style chains demonstrating the loop-forming ability of ABA-style chains and the inability of the ABC-style chains to do likewise.[70]

PDL has similarly attracted interest for use in TPEs. Lee *et al.* studied the effect of the star architecture on TPE performance of (PLLA-*b*-PDL)$_n$ block polymers while maintaining a constant overall M_n and f_{PLLA}. By increasing the number of arms from two (linear) to three, four, or six, the authors were able to demonstrate an increase in Young's moduli and tensile strength at the expense of the elongation at break.[86] The authors attributed the enhanced mechanical performance to the formation of more numerous, smaller PLLA domains embedded within the rubbery PDL matrix, which serves to increase the amount of physical cross-linking between chains.[86] As the molar mass of TPEs increases, mechanical properties typically improve, but the T_{ODT} increases. This narrows the processing window, as TPEs are generally much easier to process above their T_{ODT}. For example, Martello *et al.* found that the multiblock architecture retained high-molar mass TPE processability by decreasing T_{ODT}. At an overall molar mass of roughly 210 kg mol^{-1}, the PLLA-*b*-PDL-*b*-PLLA polymers had an inaccessible T_{ODT} while the multiblocks of the same molar mass had a T_{ODT} of 140 °C and were injection moldable.[103]

In addition to the substituted caprolactones highlighted previously, another monomer that has gained interest within PLA-block TPEs is β-methyl-δ-valerolactone (βMVL). Xiong *et al.* first made triblock polymers with PLLA end-blocks with a

https://doi.org/10.1021/acs.biomac.5c00161
Biomacromolecules 2025, 26, 2761−2783

rubbery PβMVL midblock. They found high ultimate tensile strength (28 MPa) and ductility (1720%) for a sample with f_{PLLA} = 0.32 and elastic recoveries exceeding 95% as evidenced in hysteresis testing.[152] Graft polymers with PβMVL-*b*-PLLA diblock arms were later explored by Zhang *et al.* Compared to linear PLLA-*b*-PβMVL-*b*-PLLA triblocks, the grafts of similar composition displayed nearly twice the elongation at break.[153] Siehr *et al.* further explored PβMVL-*b*-PLA based materials for their biomedical applicability. Seeking implantable devices and tissue engineering scaffolds, the authors synthesized very soft PLA-*b*-PβMVL-*b*-PLA triblocks and explored their mechanical properties both when dry and when swelled with phosphate buffered saline. They found low levels of tensile set (10−13%) after prescribed time under extension, with full recovery after 40 min for both wet and dry conditions.[154] Schüttner *et al.* also explored PLA-based block polymers for their applications as tissue engineering scaffolds. They used a novel biobased polymer, poly(citronellyl glycidyl ether carbonate) derived from CO_2 and citronellol, as the rubbery midblock. After chain extension with (−)-lactide, the polymers exhibited a desirably low modulus (0.15−1.0 MPa) and strains at break ranging from 400−650%, indicating soft materials that could be used as elastomeric tissue engineering scaffolds.[155]

Highly extensible TPEs find applications in consumer goods, automotive appliances, and biomedicine. Shin and co-workers grafted PLLA arms onto a poly(isobutylene) backbone to create "superelastomers" boasting approximately 2500% strain at break.[156] By adjusting the arm length and thereby also changing f_{PLLA}, they tuned the material properties from tough and ductile plastics to highly extensible superelastomers.[156] Highly extensible elastomers were also developed by Nakayama *et al.* by way of triblock polymers with PLLA end-blocks and a midblock comprised of PLA-*co*-PCL. These triblocks show high extensibility up to 2800% strain at break and an ultimate tensile strength of 17 MPa for a sample with f_{PLLA} = 0.20.[157] In TPEs, high extensibility typically comes at the expense of ultimate tensile strength. However, ongoing efforts seek to combine these two qualities to create incredibly tough, strong, and ductile TPEs. One key example of this is the work accomplished by Zhao *et al.*, whose materials achieved a maximum toughness of 445 MJ m^{-3} (Figure 12). Using a PCL-*co*-poly(δ-valerolactone) (δVL) rubbery midblock with PLLA end-blocks, the authors saw remarkable tensile strength (up to 71.5 MPa) and high extensibility (up to 2100%).[158] They found that while keeping the PLLA end-blocks at a constant molar mass, by increasing the rubbery midblock length they were able to improve both strain at break and ultimate tensile strength, achieving impressively high toughness values. The authors attribute the toughness of these materials to the strain-induced crystallization of the poly(εCL-*co*-δVL) midblock upon extension, as evidenced by DSC analysis of the polymer following stretching.

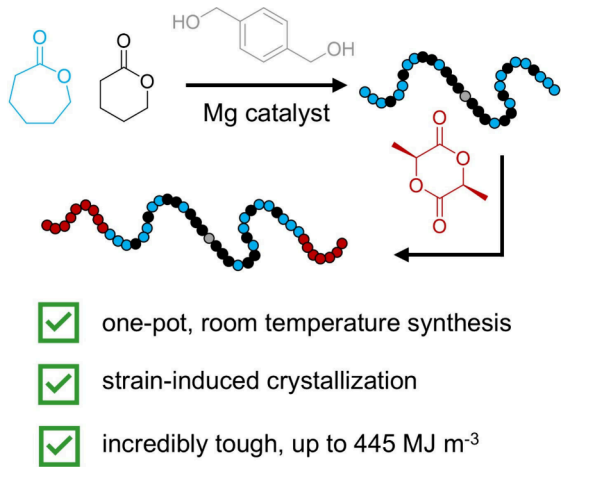

Figure 12. One-pot sequential addition of εCL/δVL and (−)-lactide with a magnesium catalyst to create triblock polymers with a gradient poly(εCL-*co*-δVL) midblock. This adapted figure has been published in CCS Chemistry 2021, ref 158.

Tough Plastics. By inverting TPE block polymer composition from low to high f_{PLA}, one produces stiff plastic materials. So far, PLA-based TPEs have been more frequently investigated than their plastic counterparts. This is mainly because commercial TPEs are neat block polymers, whereas commercial plastics are typically homopolymers or statistical copolymers. Because these plastics are most often synthesized in a one-pot fashion, the expanding portfolio of one-pot PLA block polymer syntheses[71,158−168] particularly benefits PLA block polymer plastics by demonstrating the accessibility of scaled production with existing process technologies for the respective homopolymers. Hence, with these strides in synthesis and reaction engineering underway, PLA block polymer plastics offer significant future potential by virtue of their circularity and value-adding properties.

Theryo *et al.* produced one of the earliest such materials.[169] PLA chains were grafted from a rubbery poly(1,5-cyclooctadiene-*co*-5-norbornene-2-methanol) backbone to produce a stiff, transparent, microphase separated plastic with f_{PLA} = 0.95. In tensile testing, the material showed a peculiar double yielding transition and improved ductility (238% ultimate strain), all while retaining a Young's modulus of 1.9 GPa and yield strength of 65 MPa, only slightly reduced from PLA. Later, Haugan *et al.* refined the graft architecture with PγMCL-*b*-PLA diblock grafts slightly reducing the modulus but vastly significantly extending the mechanical longevity (Figure 13).[170] Single yielding transitions were observed at low aging times in the most ductile samples, while the double yielding documented earlier by Theryo was identified as a craze-then-yield transition emergent at longer aging times. The longest-lived specimen retained an ultimate strain of 250% after 210 days of aging and a Young's modulus of ∼1.5 GPa.

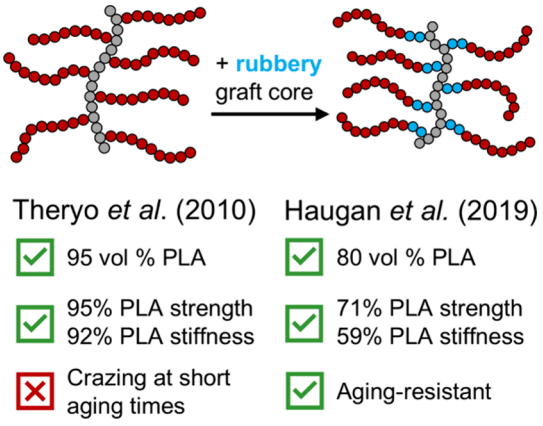

Figure 13. Adding a rubbery core block to PLA graft polymers improves aging resistance while only modestly reducing stiffness and strength.[169,170]

https://doi.org/10.1021/acs.biomac.5c00161
Biomacromolecules 2025, 26, 2761−2783

Appealing to economic feasibility, Lee *et al.* used commercially available dihydroxy-telechelic PB as macroinitiators for LBL triblocks, which they then coupled together to produce PLA−PB multiblock polymers.[104] The multiblock architecture improved toughness from PLA's typical 1−2 MJ m^{-3} to 9−170 MJ m^{-3}, though at the expense of Young's modulus and with a significant trade-off between toughness and PLA content. Mannion *et al.* observed a similar improvement when coupling PLA-*b*-PDL-*b*-PLA triblocks and $(PDL\text{-}b\text{-}PLA)_4$ star-blocks into linear and branched multiblocks, respectively.[171] The branched multiblocks strain-hardened in uniaxial extension of the melt, a desirable attribute for processability at scale. Panthani and Bates began probing the combination of PLLA crystallinity and toughness enhancement in a structurally analogous system, studying a PLLA-*b*-poly(ethylene-*co*-ethylethylene)-*b*-PLLA (LEL) triblock and its chain-extended multiblock derivative.[172] The discrete LEL was brittle like the atactic LBLs but retained typical PLLA crystallization rates. Conversely, the LE multiblock showed far superior ductility (up to 632% ultimate strain) but did not rapidly crystallize, uncovering another trade-off, this one between crystallinity and toughness. More recently, Krajovic *et al.* surmounted this trade-off in a series of PLLA-*b*-PγMCL-*b*-PLLA triblock polymers.[173] They achieved tensile toughness values ranging from 63−113 MJ m^{-3} with up to 55% PLLA crystallinity, enabling heat distortion temperatures (HDTs) exceeding those of PS, PE, and poly(propylene) (PP).

Zhang *et al.* published two studies detailing a broader scope of controlled architectural and block identity variations for optimizing properties. In the first, βMVL and (−)-lactide were sequentially grafted from a hydroxypropyl methylcellulose (HPMC) backbone to produce PβMVL-*b*-PLLA diblock graft polymers with f_{PLLA} ranging from 0.3 to 0.7.[153] This platform offered tunable (and inversely correlated) Young's modulus and ductility. Interestingly, at fixed f_{PLLA} = 0.7, doubling the length of the HPMC backbone doubled ductility without sacrificing strength. In the second, Zhang separately varied the backbone length and flexibility, grafting density, and side-chain length and composition.[174] We summarize the key trends here: (1) longer side-chains are better with fixed backbone length and side-chain composition; (2) strength correlates with f_{PLLA} for fixed backbone length; (3) a flexible backbone favors low grafting density, while a rigid backbone favors high grafting density; and (4) short, flexible backbones are best across compositions, while long, rigid backbones are best at f_{PLLA} = 0.7. These works offer opportunities for future study of the deformation mechanisms underlying these design principles.

Recent investigations have demonstrated more scalable routes to PLA block polymer plastics with excellent properties. Mulchandani *et al.* synthesized PLLA-*b*-PCL-*b*-PLLA and PDLA-*b*-PCL-*b*-PDLA triblocks, first in solvent on small scales and then in a solvent-free, one-pot, two-stage reaction on a 500g scale, removing residual lactide through sublimation.[175] The triblocks displayed high toughness (52−160 MJ m^{-3}), with one specimen notably reaching 700% ultimate strain and 36 MPa ultimate stress. Blending the triblocks improved PCL and PLLA or PDLA crystallinity owing to SC formation without appreciably affecting mechanical properties. Looking beyond melt-phase synthesis, Hong *et al.* used room temperature ball-milling to mechanochemically install atactic PLA end-blocks on a PA11 midblock, obtaining up to 98% conversion and 90% yield on a 20 g scale.[82] Then, they coupled these triblocks into linear multiblocks with a diisocyanate, again through ball-milling. Though the aging time was not reported, the resultant multiblock plastics performed very well, lacking the typical trade-off between ductility and strength while retaining PLA's yield strength (Figure 14). Finally, Dong *et al.* deconstructed commercial and

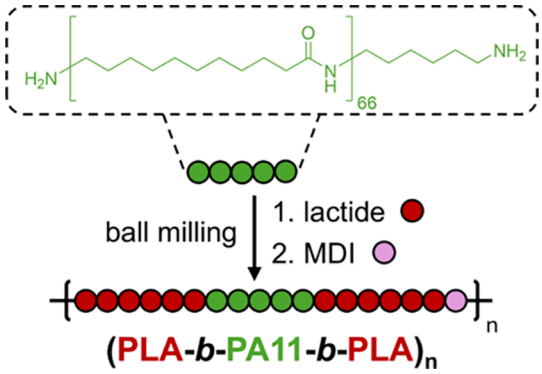

Figure 14. PLA−PA11 multiblock polymers synthesized through ball-milling show outstanding combinations of strength and ductility.[82]

postconsumer PCL and poly(butylene adipate-*co*-terephthalate) (PBAT) into controlled telechelic fragments and transesterified them into commercial PLLA, forming triblock polymers.[176] The obtained molar masses were less than 30 kg mol^{-1}, prompting diisocyanate-mediated coupling. The resultant multiblocks plastics exhibited low strengths (8−18 MPa) but extremely high ductilities (820−1150% ultimate strain) even greater than those typical of HDPE.

Blend Compatibilizers and Standalone Toughers. PLA's brittleness has spurred decades of research aiming to enhance its toughness to commercial benchmarks. Whereas the feasibility of neat block polymers as standalone plastic products depends on the scalability of developing chemistries, blending PLA with rubber is likely the most economical approach. PLA block polymers can, however, enhance these blends as compatibilizers. Due to the positive χ for most polymer pairs and their inherently low entropies of mixing, blends tend to macrophase separate into large droplets of dispersed phase within a host matrix (in this case PLA).[177] Block polymer compatibilizers incorporate a block of both the dispersed and host species, prompting localization at the droplet interfaces and increasing interfacial adhesion through coentanglement and/or cocrystallization with the blend components.[178]

More than 20 years ago, Anderson and Hillmyer explored these concepts in 80/20 PLLA/PE blends compatibilized with diblock polymers.[179] Co-crystallization of the diblock with the dispersed phase drove interfacial adhesion improvements. However, this was only helpful for toughening with a soft linear low-density PE (LLDPE) dispersed phase, which was posited to undergo cavitation to achieve high impact strength (48−75 kJ m^{-2}). On the other hand, stiff dispersed HDPE was best paired with PEP-based diblocks that could not cocrystallize, encouraging droplet debonding for the onset of matrix yielding. Thurber *et al.* more recently explored 90/10 PE/PLA blends with an attractive *in situ* reactive compatibilization approach.[180] Hydroxy-telechelic PE and $Sn(oct)_2$ catalyst were mixed into the blend, and the interfacial catalyst localization enabled rapid transesterification of the HO−PE−OH into the dispersed PLA backbones, forming triblock compatibilizers. Although this was a PLA-lean blend, this compatibilizer synthesis scheme would, in principle, also

https://doi.org/10.1021/acs.biomac.5c00161
Biomacromolecules 2025, 26, 2761−2783

pertain to PLA-rich blends. Hong *et al.* again employed ball mill synthesis to produce PA11-PLA diblocks, triblocks, and linear multiblocks as compatibilizers for 70/30 PLA/PA11 blends.[181] Concurrent PA11 cocrystallization and PLA coentanglement produced the best properties, including greater than 50 MPa tensile strength with ultimate strains of over 400% similar to the neat block polymers.

PLLA/PDLA stereocomplexation has been employed in PLA enhancement for decades.[182] Though SC use in PLA blend compatibilization has only recently popularized, it has quickly emerged as a key design element for the highest-performing materials on record. For example, in 2019 Wu *et al.* prepared 68/20/12 PLLA/EVMG/PDLA blends (EVMG = ethylene-vinyl acetate-glycidyl methacrylate copolymer elastomer).[183] Mixing the three components in a ternary blend produced mostly free PDLA chains (*i.e.*, not bound to EVMG), while first blending EVMG/PDLA to isolate the grafting-to reaction and then blending the EVMG-*g*-PDLA product into PLLA led to mainly EVMG bound PDLA chains. The latter approach was far superior, transforming the blend morphology from "sea−island" (droplet in matrix) to cocontinuous PLLA/EVMG and producing an impact strength of 93.2 kJ m^{-2}, an 84-fold improvement upon PLLA.

This theme of interface-anchored PDLA chains inducing transitions to cocontinuous host/dispersed morphologies has since hallmarked the state-of-the-art. Chen *et al.* created fully biorenewable 70/30 PLLA/PBAT blends compatibilized with a PDLA/PBAT-based graft polymer made *ex-situ* as with the EVMG-based blend.[184] With careful PLLA-based compatibilizer and free PDLA controls, they showed that a thermally stable cocontinuous morphology resulted specifically from interface-localized SCs. The best blend displayed an impact strength of 53 kJ m^{-2}, 350% ultimate strain, and 45 MPa ultimate stress. By choosing poly(epichlorohydrin) (PECH) for the dispersed phase in 80/20 PLLA/PECH blends compatibilized with PECH-*b*-PDLA diblocks, Chen *et al.* combined rubbery dipolar interactions with interfacial stereocomplexation (Figure 15).[185] With just 5 wt % compatibilizer, the blend achieved an impact strength of 87 kJ m^{-2}, 568% ultimate strain, and 53 MPa ultimate stress. Increasing the diblock loading to 15 wt % reduced ductility to 100% ultimate strain but produced the highest recorded impact strength for a PLA-rich compatibilized blend, 96 kJ m^{-2}. Most recently, Li *et al.* created PBAT-*g*-PDLA for similar use in 70/30 PLLA/PBAT blends, importantly clarifying that the transition to cocontinuous morphology is driven solely by *in situ* SC formation and not by intrinsic phase inversion processes governed by the components' viscosity ratio.[186,187]

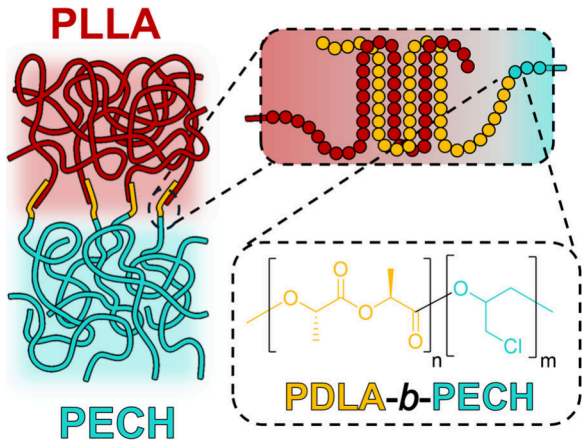

Figure 15. Using PECH-*b*-PDLA diblocks as compatibilizers for 80/20 PLLA/PECH blends achieves excellent strength, ductility, and the highest recorded impact strength for a PLLA-based blend.[185]

Finally, we highlight three examples in which PLA block polymers were used as standalone toughening − added directly to PLA hosts without other dispersed phases. Depending on the comparative cost of rubber and the block polymer, this PLA upgrading method could be the most cost-effective at low loadings of block polymer. Lee *et al.* grafted PγMCL-*b*-PLA diblocks from a hydroxyl-functionalized backbone similarly to Haugan *et al.*, expanding the architectural scope to 3- and 4-arm star backbones.[188] After blending into PLA, the linear backbone with 40 grafts per arm and the 3- and 4-arm star molecules, each with 10 grafts per arm, were equally effective tougheners at 5 wt % loading, enabling toughnesses of ∼90 MJ m^{-3} without reducing Young's modulus. Increasing block polymer content delayed host aging; ductility was retained for up to 107 days at 20 wt % loading. Interested in leveraging SCs, Wang *et al.* compared blends 5−15 wt % composites of linear PLA-*b*-PB and PDLA-*b*-PB multiblock polymers in a PLLA host.[189] At 5 wt %, PDLA-*b*-PB multiblocks provided more ductility than the amorphous PLA-*b*-PB variety and provided nearly twice the strength at 15 wt %, which was ascribed to a SC-mediated physical cross-linking effect. Nattawut *et al.* used an $Sn(OMe)_2$ catalyst's switchable kinetics for ROCOP and (−)-lactide ROTEP to create [poly(maleic anhydride)-*stat*-poly(propylene oxide)]-*b*-PLLA polymers.[190] After mild thiol−ene cross-linking over the maleic anhydride alkene units, at just 2 wt % loading, these additives achieved a 4-fold increase in the tensile toughness of commercial PLLA without decreasing Young's modulus.

FUTURE PERSPECTIVES

A vision of circularity for the future polymer industry of course demands scientific strides beyond the advancements cataloged here. As the synthetic "bioplastic" nearest to megatonne-scale production, PLA will continue to play a major part in driving the transition to renewable and degradable polymeric materials. Much of the work recounted here shows what is possible for PLA-based materials, while many fewer address themes associated with translating fundamental discoveries into practical, scalable PLA-based materials. Societal impact further requires moving from what is practical to what is economically and environmentally profitable. Thus, technoeconomic analysis and full life cycle assessment (LCA) are necessary to move technologies into the marketplace to achieve this 2-fold goal. We conclude our Perspective calling attention to specific themes that we posit should receive attention in the coming years given the urgency of the quest for a circular economy.

Maintaining Sufficient, Market-Conscious Circularity. The global biomaterials policy landscape has primed demand for competitive, fully circular materials. The European Union's (EU) legislative efforts toward circularity include taxing of nonrecycled plastic packaging waste,[191] restricting the use of disposable plastic bags,[192] and banning single-use plastics lacking renewable substitutes.[193] Moreover, in 2022 the European Commission enacted a policy framework[194] for "biobased, biodegradable, and compostable plastics" that recommends application areas based on life cycle topology − biosourced, compostable, or both − and references the

https://doi.org/10.1021/acs.biomac.5c00161
Biomacromolecules 2025, 26, 2761−2783

Ecodesign for Sustainable Products Regulation (ESPR) law[195] for guidance on prioritizing renewables investments. The ESPR therefore provides a useful rubric for determining the market relevance of ongoing PLA research. Several EU members have enacted extended producer responsibility (EPR) laws, which charge plastics manufacturers with postconsumer product stewardship and incentivize sustainable end-of-life management.[196] Across the Asia-Pacific Economic Cooperation, Chile, Japan, Thailand, and Malaysia have passed similar EPR laws and defined scope and regulations for bioplastics.[197] Seven U.S. states have passed EPR or similar laws for plastics, and 10 more states have EPR bills under consideration.[198,199] Two recent reports by the U.S. Office of Science and Technology Policy and the Department of Agriculture outline an ambitious goal of 90% sustainable replacement of current commercial polymers within 20 years and a roadmap to growing the biomass supply for renewable plastics.[200,201]

Compostability of products that contain PLA is also an important consideration. In North America, the Biodegradable Products Institute (BPI) leads third-party certification of compostability for product labeling and sorting. BPI certification minimally requires compliance with the American Society for Testing and Materials (ASTM) standard D6400 for bulk plastics or D6868 for products incorporating plastics as coatings or additives. These standards stipulate that nominally compostable products must (1) demonstrate 90% conversion of organic carbon to CO_2 in 180 days under industrial composting conditions standardized in ASTM D5338;[202] (2) contain 5 wt % or less of organic constituents not yet verified under D6400 or D6868, with each constituent not exceeding 1 wt %; and (3) not contain more than 10 wt % of any organic constituent that fails to satisfy item (1).[203,204] In Europe, the leading standard EN 13432 requires (1) 90% disintegration in 12 weeks; (2) 90% conversion of organic carbon to CO_2 within six months; and a lack of (3) adverse effects on the composting process, (4) heavy metals, and (5) perturbation of the chemical characteristics of the resultant compost.[205] These criteria would likely immediately disqualify many of the materials described in this Perspective, whether for contents of nondegradable blocks above 10 wt % or, in some cases, for use of transition metal catalysts that would not be recovered at scale. Compostability standards constrain plastics manufacturers, but compostability certification does not guarantee that consumers will have industrial compost infrastructure available or will comply with associated requirements. Analysis of food waste collected for composting shows 9−13 wt % contamination by improper materials, the plurality being nondegradable, single-use plastic packaging and household goods.[206] LCA[206] and agricultural experiments[207,208] show that these contaminants pose ecological and economic harms to the organismal and human communities involved.

Depending on the technological context, there may be no realistic sustainability benefit to incorporating PLA with moderate-to-high weight fractions of nondegradable polymers. For instance, when PLA is used as a substitute for PS glassy blocks in TPEs, composting is unrealistic if the rubbery block is not designed for biodegradability. Likewise, when targeting tough plastics, including nondegradable ingredients at more than 10 wt % loading precludes compostability, whereas loadings of 20−30 wt % have typically achieved the best balance of competitive properties in the existing literature. In these cases, the benefit to using PLA would thus come from its biorenewable sourcing, as the greenhouse gas (GHG) emissions for in-use operations including manufacturing and processing have been reported to be similar among PLA and polyolefins.[209] However, when considering the GHG emissions associated with PLA degradation under industrial composting or in landfill, the latter deleteriously converting 50% of PLA carbon to methane,[210] the most optimized production of Ingeo PLA by NatureWorks LLC[211] suggests that landfilled PLA has the same total GHG emissions as HDPE (2.6 kg CO_2-eq kg^{-1}), while composted PLA incurs only 0.4 kg CO_2-eq kg^{-1} less.[209] Moreover, if we choose to assess environmental impact by other metrics, such as land and water use, petroleum-derived plastics are less burdensome.[212] If not motivated by LCA, the decision to arbitrarily incorporate PLA into any given product does not "displace" nonrenewable thermoplastics from the materials economy. Commodity plastics (HDPE, 1.01 USD kg^{-1}; LLDPE, 0.94 USD kg^{-1}; LDPE, 1.24 USD kg^{-1}; PP, 1.20 USD kg^{-1}; PET, 1.52 USD kg^{-1}; PS, 1.36 USD kg^{-1}; PVC, 0.93 USD kg^{-1}; North American prices current as of March 2025) currently have such a large price point advantage over PLA (2.42 USD kg^{-1}) and other biorenewable plastics that their demands are essentially independent.[213−218] That is, while PLA production capacity is accelerating, it has little to no impact on the size or trajectory of petro-plastic markets. But when viewed in parallel with the aforementioned policy measures, as well as mounting consumer preference for ecologically benign materials,[219,220] increasing PLA presence across the thermoplastics market will help to motivate further increases in its production capacity toward the crucial goal of cost-competitiveness. If PLA becomes as affordable as polyolefins, its demand may surge in a wide array of markets.

Thus, taking stock of these constraints, we must clearly understand target markets for new PLA-containing materials and carefully choose the identity and content of non-PLA components accordingly. The optical transparency or translucency of neat PLA block polymer plastics (Tough Plastics) and PLA blends with standalone tougheners (end of Blend Compatibilizers and Standalone Tougheners) naturally suggests their candidacy for replacing HDPE, LLDPE, PP, PS, and PET in single-use applications. Because single-use products are landfilled or leak into the environment at the highest rates, it is particularly essential to preserve the route to a sustainable end-of-life by using compostable co-blocks in such applications. Underused biomass waste feedstocks for co-blocks or comonomers should be prioritized, including lignocellulosics, agricultural waste, and microalgae.[221−223] As part of these investigations, directly verifying compostability using ASTM D5338 is most preferable, though the entailed requirements of time (6 months), material (∼100 g), and instrumentation (respirometers or online gas chromatographs) limit the accessibility of this method. To address these hurdles, da Silva *et al.* constructed an inexpensive in-house Bartha respirometer and stimulated their compost inoculum with yeast, reducing the biodegradation time to 28 days while using only 0.25 g of each polymer sample and qualitatively matching results from ASTM D5338.[224] Further progress in accelerated composting will afford PLA block polymer researchers a more tractable route to comprehensively assessing their materials' circularity potential. Given the lack of formal third-party standardization for accelerated testing, these protocols must be replicated as consistently as possible across different laboratories.

Conversely, when using or validating compostable co-blocks is not feasible, we should target products for the highest-value,

https://doi.org/10.1021/acs.biomac.5c00161
Biomacromolecules 2025, 26, 2761−2783

lowest-volume, longest-lifetime applications possible, such as engineering plastics and high-performance elastomers and adhesives. This will slow the influx of PLA materials into unsustainable end-of-life pathways and further supply the portfolio of advanced sustainable materials to deploy when economically permissible. For instance, the currently highest performing compatibilized PLA blends have comparable properties to several engineering plastics (Table S2). Conveniently, optical transparency is a less frequent requirement for engineering plastics, and most PLA blends are opaque due to large droplet sizes and refractive index mismatch between PLA and the dispersed phase. PLA block polymer research is needed for increasingly sophisticated compatibilizers that offer parity on processability and in-use properties. Recently, PLA blends with biodegradable dispersed phases, including PBAT and poly(butylene succinate),[184,186,225] have emerged as high-performing materials when loaded with at least 5 wt % compatibilizer. Considering the constraints we have discussed, reducing the required compatibilizer loading to 1 wt % would achieve substantial benefits. The product would be cheaper, comply with compostability regulations, and extend the synthetic scope for compatibilizers to nonrenewable co-blocks, which could itself further reduce costs. Success in this endeavor could inspire a new market for high-value, fully circular engineering plastics.

Scalability. We must choose safely and economically scalable chemistries for PLA block polymers if they are to be feasible in a future circular economy. In commercial production, PLA and other thermoplastics are synthesized in bulk with the highest permissible catalyst loadings for the fastest practical throughput at maximum monomer conversion. These products often contain residual monomer and catalyst, and they tend to have considerably higher molar mass dispersities than those desirable for academic structure−property studies. If the favorable properties discovered for a material in its target market crucially depend on low molar mass dispersity, well-defined microstructure, and extensive purification, then it has dubious technical relevance.

In the tough plastics space, PLA materials blended with rubber or standalone tougheners are advantageous in this view, as the high-cost block polymers are included at low weight fractions, and the preparation only involves melt-blending them with commercial materials. Neat PLA-rich block polymers, however, face more stringent requirements. Ideally, these syntheses would take place in a one-pot method. Depending on the block synthesis order, this would require miscibility between the co-block and lactide or between PLA and the comonomer. The comonomers would ideally have ceiling temperatures compatible with bulk lactide polymerizations, which are typically carried out between 140 and 180 °C. Sufficient lactide purity would also be crucial. The higher the molar mass of a targeted PLA block, the more likely are impurities within the lactide to adventitiously initiate impurity homopolymer chains in competition with the intended initiator.[173] Because plastics require large PLA molar masses relative to co-blocks, impurity-rich lactide could produce excessively short PLA blocks and compromise mechanical properties. As detailed earlier, molar mass dispersity can impact self-assembled block polymer morphology, and so the precise morphologies obtained may be impacted by polymerization method. Hence, the most commercially actionable approaches will verify (in)compatibility between PLA and the co-block (or comonomer), identify tractable lactide purification methods, and confirm property retention after bulk synthesis.

In the case of TPEs with lower PLA content, synthetic requirements might be easier and more technologically disruptive. Controlled anionic polymerization is used for commercial production of TPEs derived from fossil resources.[226] This technique's inherent sensitivity to impurities and the entailed constraints on polymerization conditions complicate large-scale production.[227] Here, one-pot synthetic capabilities for the synthesis of renewable, rubbery midblocks and subsequent chain extension with lactide are advantageous. The monomers that give low glass transition polymers are often liquids at room temperature, allowing purification through distillation. Lactide purity requirements are also less stringent due to the lower PLA content.

Postreaction purification at scale should not be overlooked. Devolatilization of residual monomer and solvent is commonplace in industry,[228] and therefore light comonomers are favorable considering the success of sublimation in removing lactides.[175,229] $Sn(oct)_2$ catalyst is generally not removed from commercial PLA products, and so tin(II)-active lactone comonomers are attractive for one-pot reactions. In light of the current discomfort with using tin-based reagents, dimethyl phosphonic acid[149] and HCl[230,231] are also useful for ROP of lactone comonomers and are easily devolatilized.

Crucial Property Testing. *Processability.* High-throughput melt processing operations benefit from three material attributes: shear thinning, extensional thickening, and rapid crystallization for crystallizable components. If a PLA blend or block polymer has a much greater shear viscosity than PLA homopolymer, efficient processing would require higher temperatures, which could pose risks of PLA degradation when higher than about 200 °C for prolonged periods. Dispersed components in blends and composites tend to increase shear viscosity, especially rigid materials such as cellulose nanofibers[232,233] and carbon fibers.[234] In these cases, it is worthwhile to evaluate the viscosity-temperature relationships within the processing window (along with thermogravimetric analyses to assess PLA thermal stability) and with respect to viscosities of commercial materials in the target market. Extensional thickening, characterized by a rapid increase in the transient extensional viscosity during melt extension, facilitates film blowing, extrusion blow-molding, and thermoforming.[235,236] Not all grades of commercial linear PLA thicken in extension, and so there is opportunity to generally improve PLA melt strength by using nonlinear block polymer architectures[91,237,238] and by including both PLLA and PDLA blocks to generate SCs.[239] While SCs are also useful as nucleating agents to address PLLA's slow crystallization, they have the often overlooked drawback of enhanced hydrolytic stability, which can hinder industrial composting.[240,241] Alternatively, low weight fractions of well-dispersed, bioderived nucleating agents[242,243] should be investigated as complements to rubbery homopolymers or co-blocks to produce compostable, tough, fast crystallizing materials.

Thermal Resilience As Processed. Most research articles on PLLA upgrading make some mention of its slow crystallization kinetics, and some target acceleration strategies as part of the original work. Increasing the maximum service temperature (MST) of as-processed parts is the ultimate (but sometimes unmentioned) goal of accelerating PLLA crystallization. While the MST is often empirically defined, the HDT and Vicat softening temperature (VST) are the most common proxies

https://doi.org/10.1021/acs.biomac.5c00161
Biomacromolecules 2025, 26, 2761−2783

measurable at lab scales for plastics. Under constant load at controlled heating rates, the HDT marks a flexural deflection threshold,[244,245] while the VST marks a depth of flat needle penetration.[246] We note the ease of HDT measurement according to ASTM E2092-23: specimens with minimal dimensions of 12 × 10 × 1 mm are typical, requiring only 150 mg of PLA. However, conventional analyses of thermal resilience − the second heating crystallinity measured with dynamic DSC, the isothermal crystallization half-time, the crystallite nucleation density measured with polarized optical microscopy, and the plateau storage modulus above $T_{g,\,PLLA}$ measured with dynamic mechanical thermal analysis − rationalize, but do not directly inform, market readiness. It is also worth noting that meaningfully increasing PLLA's HDT requires achieving at least 40% crystallinity.[247] Therefore, it is essential to measure the first heating crystallinity (or HDT) of mechanical specimens as processed. Adopting this perspective will help identify and refine the most promising, crystallinity-tolerant mechanical enhancements.

In TPEs, the high melting point of PLLA ($T_m \approx 170-180$ °C) or its SC with PDLA ($T_m \approx 220-230$ °C) could also provide a thermal resilience advantage over the incumbent styrenic TPEs with hard segment resilience limited by $T_{g,\,PS} \approx 100$ °C.[248] These high melting points position PLA-based materials in the highest tiers of TPE thermal stability, which is especially beneficial for biomedical applications, where steam sterilization is preferred.[249]

Aging Resistance. Physical aging refers to the contraction of free volume that occurs below T_g as chain motion gradually reconfigures the molecules into lower free energy states relative to the initial nonequilibrium glass.[250] PLA dramatically embrittles *via* this mechanism over just 48 h of room temperature aging, with typical strains at break decreasing from over 250% to less than 10% over that time period.[251] In typical plastic life cycles, the time elapsed between the original processing and consumer use of a product could span weeks to months. However, treatments of physical aging in enhanced PLA materials are rare in the literature, most often appearing only when research specifically aims to engineer aging resistance into the material. Measuring excellent mechanical properties after 24 or 48 h of aging, which are the most commonly reported aging times, does not guarantee that these properties will persist for weeks, let alone months, to serve in use.[170,188] This is especially important when targeting engineering plastic markets, as these products' service durations far exceed those of single-use plastics. Failing to report aging time obscures materials' technical relevance given the extreme age-sensitivity of PLA's toughness. Figure 16 displays the reported tensile properties of all PLA block polymer plastics reviewed in this Perspective as functions of aging time (symbols) and total PLA weight fraction (color). Casting the metrics in this way shows the property ranges offering the highest PLA valorization potential (*i.e.*, the highest w_{PLA}), as well as the aging time's influence on mechanical properties. Materials richer in PLA tend to have higher strength and stiffness, though at the expense of ductility and toughness due to the inherently greater potential for physical aging. Note the high frequency of materials on the frontier of both strong and ductile (Figure 16a) or both stiff and tough (Figure 16b) that lack a reported aging time. Thus, inconsistencies in reports of aging also make it difficult to definitively identify property bottlenecks and breakthroughs to inform future research. We must more consistently perform

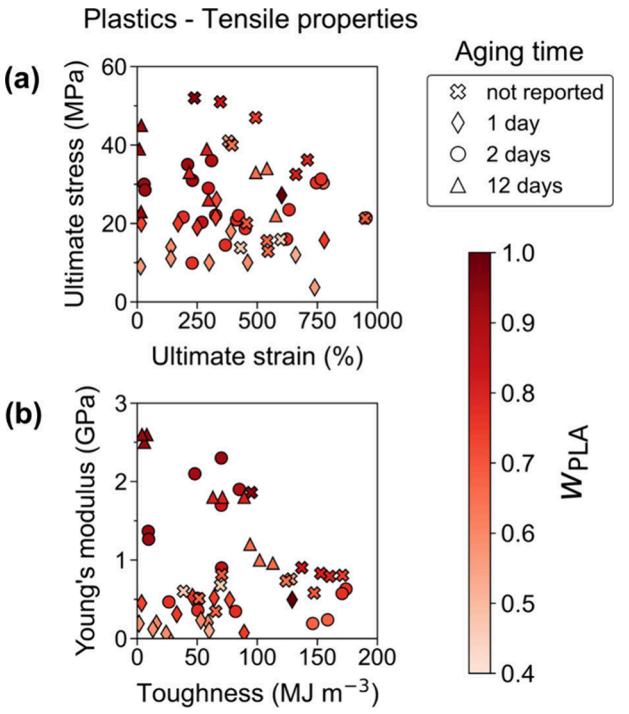

Figure 16. Compiled tensile properties of PLA-based block polymer plastics highlighted in this Perspective. The marker style indicates reported aging time (or lack thereof), and the color indicates the total weight fraction of PLA in the material.

mechanical testing on specimens of advanced physical age to sidestep pitfalls in material design, making sure to report an aging time alongside every property measured.

Optical Transparency. The automotive, aerospace, athletic, and other industries often face a trade-off between optical transparency and desirable mechanical properties in high-performance parts. Inorganic and polymeric glasses are transparent but lack the toughness and strength required to withstand mechanical challenges in use, such as scratches and impact forces.[252] Conversely, compositing glassy polymers with rubber provides toughness but often reduces optical clarity due to the refractive index mismatch between the host and dispersed phase. Decreasing the dispersed phase particle diameters below 40 nm sufficiently reduces their Rayleigh scattering of visible light wavelengths to achieve transparency. PLA block polymers easily accomplish this task owing to the nanoscale self-assembly of block domains, which typically have dimensions ranging from 5 to 50 nm. But in polymer blends, which currently have more promise for engineering plastic applications than neat block polymers, interfacial tensions between host and dispersed polymers lead to typical particle sizes between 200 and 1000 nm.[253] Instead of reducing the scatterer size, the next approach is to reduce the scattering contrast by matching the components' refractive indices. A popular commercial example is MABS (methyl methacrylate acrylonitrile butadiene styrene), in which methyl methacrylate is incorporated into the acrylonitrile-styrene copolymerization to better match the refractive indices of the stiff ABS matrix and PB droplets. In this case, the methyl methacrylate content must be carefully controlled so as not to compromise toughness.[254] Therefore, the discovery of renewable, rubbery polymers closely or fully index-matched with PLA will be

https://doi.org/10.1021/acs.biomac.5c00161
Biomacromolecules 2025, 26, 2761−2783

instrumental in helping compatibilized PLA blends keep pace with property demands in the engineering plastics market.

SUMMARY

The vast field of polymer science and technology has grown immensely in the past century, fueled by the desire to meet the needs of a growing world population. As such, the world has been inundated with plastic products from the convenient (*e.g.*, diapers, grocery bags, cell phones), to the life-saving (*e.g.*, IV bags, medical tubing, pharmaceuticals), to the extraordinary (*e.g.*, airplane parts, prosthetic limbs, computers). However, in meeting the needs of the here and now, less attention to the needs of future generations has been given. Despite bleak projections regarding the state of plastic pollution, we must maintain the pace of sustainability innovation to support the most aggressive pollution-reducing strategy, the System Change Scenario.[26,255,256]

While bioplastics remain currently less than 1% of global plastic production, this number is certain to increase in coming years as governmental policies seek to stem the flow of unsustainable plastics into the environment. As the largest share of that meek percentage, PLA shows promise as a bioplastic for its ability to be biosourced and its propensity toward degradation in industrial composting facilities. While its merits are manyfold, the use of PLA within everyday applications requires more technological advancements to truly harness its useful properties. One such way through which this will be accomplished is the development, scale-up, and production of block polymers containing PLA segments.

ASSOCIATED CONTENT

Supporting Information

The Supporting Information is available free of charge at https://pubs.acs.org/doi/10.1021/acs.biomac.5c00161.

Bar graph indicating number of citations for PLA block polymers over time, descriptions of χ_{eff} determination methods referenced in Table 1, and property comparison of select PLA block polymer blends with common engineering plastics (PDF)

AUTHOR INFORMATION

Corresponding Author

Marc A. Hillmyer − *Department of Chemistry, University of Minnesota, Minneapolis, Minnesota 55455, United States;* orcid.org/0000-0001-8255-3853; Email: hillmyer@umn.edu

Authors

Daniel M. Krajovic − *Department of Chemical Engineering and Materials Science, University of Minnesota, Minneapolis, Minnesota 55455, United States;* orcid.org/0000-0001-5311-1941

Margaret S. Kumler − *Department of Chemistry, University of Minnesota, Minneapolis, Minnesota 55455, United States;* orcid.org/0000-0003-2494-6135

Complete contact information is available at: https://pubs.acs.org/10.1021/acs.biomac.5c00161

Author Contributions

D.M.K.: Outlining, drafting, writing, editing, figure conceptualization and preparation, and logistical coordination. M.S.K.: Outlining, drafting, writing, editing, figure conceptualization and preparation, and logistical coordination. M.A.H.: Conceptualization, project coordination, review, editing, and writing.

Notes

The authors declare the following competing financial interest(s): Marc A. Hillmyer is a cofounder of Valerian Materials. He has equity and royalty interests in and serves on the Board of Directors of Valerian Materials, a company involved in the commercialization of beta methyl valerolactone. The University of Minnesota also has equity and royalty interests in Valerian Materials. These interests have been reviewed and managed by the University of Minnesota in accordance with its Conflict-of-Interest policies.

Biographies

Daniel M. Krajovic grew up in Pennsylvania and received his B.S. in Chemical Engineering from the University of Rochester in 2020. He is currently a Ph.D. candidate in Chemical Engineering at the University of Minnesota, Twin Cities.

Margaret S. Kumler grew up in California and received her B.S. in Chemistry from California Polytechnic State University, San Luis Obispo. She is currently a Ph.D. candidate in Chemistry at the University of Minnesota, Twin Cities.

Marc A. Hillmyer grew up in Florida and received his B.S. in Chemistry from the University of Florida in 1989 and his Ph.D. in Chemistry from the California Institute of Technology in 1994. He is currently the McKnight Presidential Endowed Chair in Chemistry and the Director of the Center for Sustainable Polymers at the University of Minnesota, Twin Cities.

ACKNOWLEDGMENTS

We thank the National Science Foundation (NSF) for financial support through a grant from the Division of Chemistry (CHE-2403983). D.M.K. acknowledges funding from a University of Minnesota College of Science and Engineering Fellowship and an NSF Graduate Research Fellowship (Grant 2237827). M.S.K. acknowledges funding from a 3M Science and Technology Graduate Fellowship and an NSF Graduate Research Fellowship (Grant 2237827). We also thank Dr. Peter V. Kelly, Dr. Arron C. Deacy, and Dr. Jonathan P. Coote for reviewing drafts of this Perspective prior to submission.

REFERENCES

(1) Andrady, A. L.; Neal, M. A. Applications and Societal Benefits of Plastics. *Philos. Trans. R. Soc. B Biol. Sci.* **2009**, *364* (1526), 1977−1984.
(2) Our History. *Kraton About*. https://kraton.com/about/#history (accessed 2024-12-16).
(3) Jambeck, J. R.; Geyer, R.; Wilcox, C.; Siegler, T. R.; Perryman, M.; Andrady, A.; Narayan, R.; Law, K. L. Plastic Waste Inputs from Land into the Ocean. *Science* **2015**, *347* (6223), 768−771.
(4) Geyer, R.; Jambeck, J. R.; Law, K. L. Production, Use, and Fate of All Plastics Ever Made. *Sci. Adv.* **2017**, *3* (7), No. e1700782.
(5) de Souza Machado, A. A.; Kloas, W.; Zarfl, C.; Hempel, S.; Rillig, M. C. Microplastics as an Emerging Threat to Terrestrial Ecosystems. *Glob. Change Biol.* **2018**, *24* (4), 1405−1416.
(6) Napper, I. E.; Davies, B. F. R.; Clifford, H.; Elvin, S.; Koldewey, H. J.; Mayewski, P. A.; Miner, K. R.; Potocki, M.; Elmore, A. C.; Gajurel, A. P.; Thompson, R. C. Reaching New Heights in Plastic Pollution—Preliminary Findings of Microplastics on Mount Everest. *One Earth* **2020**, *3* (5), 621−630.
(7) Chatterjee, S.; Sharma, S. Microplastics in Our Oceans and Marine Health. *Field Actions Sci. Rep. J. Field Actions* **2019**, *19*, 54−61.

(8) Puskic, P. S.; Lavers, J. L.; Bond, A. L. A Critical Review of Harm Associated with Plastic Ingestion on Vertebrates. *Sci. Total Environ.* **2020**, *743*, No. 140666.
(9) *bp Energy Outlook, 2023 Edition*; bp Energy Economics, 2023.
(10) *The New Plastics Economy: Rethinking the Future of Plastics*; World Economic Forum, 2016.
(11) Groot, W.; van Krieken, J.; Sliekersl, O.; de Vos, S. Production and Purification of Lactic Acid and Lactide. In *Poly(Lactic Acid)*; John Wiley & Sons, Ltd., 2022; pp 1−18. DOI: 10.1002/9781119767480.ch1.
(12) Masutani, K.; Kimura, Y. PLA Synthesis. From the Monomer to the Polymer. In *Poly(lactic acid) Science and Technology*; Polymer Chemistry Series; Royal Society of Chemistry, 2014; pp 1−36. DOI: 10.1039/9781782624806-00001.
(13) Gruber, P. R.; Hall, E. S.; Kolstad, J. J.; Iwen, M. L.; Benson, R. D.; Borchardt, R. L. *Continuous Process for the Manufacture of a Purified Lactide from Esters of Lactic Acid.* US5247059A, 1993.
(14) Farah, S.; Anderson, D. G.; Langer, R. Physical and Mechanical Properties of PLA, and Their Functions in Widespread Applications — A Comprehensive Review. *Adv. Drug Delivery Rev.* **2016**, *107*, 367−392.
(15) Tyler, B.; Gullotti, D.; Mangraviti, A.; Utsuki, T.; Brem, H. Polylactic Acid (PLA) Controlled Delivery Carriers for Biomedical Applications. *Adv. Drug Delivery Rev.* **2016**, *107*, 163−175.
(16) Farrington, D. W.; Lunt, J.; Davies, S.; Blackburn, R. S. 5 - Poly(Lactic Acid) Fibers (PLA). In *Polyesters and Polyamides*; Deopura, B. L., Alagirusamy, R., Joshi, M., Gupta, B., Eds.; Woodhead Publishing Series in Textiles; Woodhead Publishing, 2008; pp 140−170. DOI: 10.1533/9781845694609.1.140.
(17) Domenek, S.; Courgneau, C.; Ducruet, V. Characteristics and Applications of Poly(Lactide). In *Biopolymers: Biomedical and Environmental Applications*; Scrivener Publishing, 2011.
(18) *Bioplastics Market Development Update 2023*; European Bioplastics, 2023.
(19) *21 CFR 175.300 -- Resinous and polymeric coatings*. https://www.ecfr.gov/current/title-21/part-175/section-175.300 (accessed 2024-06-25).
(20) FCN No. 475. *NatureWorks LLC*; U.S. Food and Drug Administration, 2005. https://www.hfpappexternal.fda.gov/scripts/fdcc/index.cfm?set=FCN&id=475.
(21) Swetha, T. A.; Bora, A.; Mohanrasu, K.; Balaji, P.; Raja, R.; Ponnuchamy, K.; Muthusamy, G.; Arun, A. A Comprehensive Review on Polylactic Acid (PLA) − Synthesis, Processing and Application in Food Packaging. *Int. J. Biol. Macromol.* **2023**, *234*, No. 123715.
(22) Gorrasi, G.; Pantani, R. Hydrolysis and Biodegradation of Poly(Lactic Acid). In *Synthesis, Structure and Properties of Poly(lactic acid)*; Di Lorenzo, M. L., Androsch, R., Eds.; Springer International Publishing: Cham, 2018; pp 119−151. DOI: 10.1007/12_2016_12.
(23) Li, Y.; Tao, L.; Wang, Q.; Wang, F.; Li, G.; Song, M. Potential Health Impact of Microplastics: A Review of Environmental Distribution, Human Exposure, and Toxic Effects. *Environ. Health* **2023**, *1* (4), 249−257.
(24) Lott, C.; Stemmer-Rau, K.; Weber, M. *PeToPLA: A Meta-Study on the Persistence and Toxicity of PLA, and the Formation of Microplastics in Various Environments*; HYDRA Marine Sciences; GMBH, 2024.
(25) *Bioplastics Market Development Updates, 2016−2024*; European Bioplastics.
(26) *Breaking the Plastic Wave: A Comprehensive Assessment of Pathways Towards Stopping Ocean Plastic Pollution; The Pew Charitable Trusts*; SYSTEMIQ, 2020.
(27) Feng (S. T. Voong), X. D.; Song, C. X.; Chen, W. Y. Synthesis and Evaluation of Biodegradable Block Copolymers of ε-Caprolactone and DL-Lactide. *J. Polym. Sci. Polym. Lett. Ed.* **1983**, *21* (8), 593−600.
(28) Song, C. X.; Sun, H. F.; Feng, X. D. Microspheres of Biodegradable Block Copolymer for Long-Acting Controlled Delivery of Contraceptives. *Polym. J.* **1987**, *19* (5), 485−491.
(29) Younes, H.; Cohn, D. Morphological Study of Biodegradable PEO/PLA Block Copolymers. *J. Biomed. Mater. Res.* **1987**, *21* (11), 1301−1316.
(30) Younes, H.; Nataf, P. R.; Cohn, D.; Appelbaum, Y. J.; Pizov, G.; Uretzky, G. Biodegradable Pela Block Copolymers: In Vitro Degradation and Tissue Reaction. *Biomater. Artif. Cells. Artif. Organs* **1988**, *16* (4), 705−719.
(31) Leenslag, J. W.; Pennings, A. J. Synthesis of High-Molecular-Weight Poly(L-Lactide) Initiated with Tin 2-Ethylhexanoate. *Makromol. Chem.* **1987**, *188* (8), 1809−1814.
(32) Witzke, D. R.; Narayan, R.; Kolstad, J. J. Reversible Kinetics and Thermodynamics of the Homopolymerization of L-Lactide with 2-Ethylhexanoic Acid Tin(II) Salt. *Macromolecules* **1997**, *30* (23), 7075−7085.
(33) Thurn-Albrecht, T.; Schotter, J.; Kästle, G. A.; Emley, N.; Shibauchi, T.; Krusin-Elbaum, L.; Guarini, K.; Black, C. T.; Tuominen, M. T.; Russell, T. P. Ultrahigh-Density Nanowire Arrays Grown in Self-Assembled Diblock Copolymer Templates. *Science* **2000**, *290* (5499), 2126−2129.
(34) Crossland, E. J. W.; Ludwigs, S.; Hillmyer, M. A.; Steiner, U. Freestanding Nanowire Arrays from Soft-Etch Block Copolymer Templates. *Soft Matter* **2007**, *3* (1), 94−98.
(35) Zalusky, A. S.; Olayo-Valles, R.; Taylor, C. J.; Hillmyer, M. A. Mesoporous Polystyrene Monoliths. *J. Am. Chem. Soc.* **2001**, *123* (7), 1519−1520.
(36) Hampu, N.; Hillmyer, M. A. Molecular Engineering of Nanostructures in Disordered Block Polymers. *ACS Macro Lett.* **2020**, *9* (3), 382−388.
(37) Hampu, N.; Werber, J. R.; Chan, W. Y.; Feinberg, E. C.; Hillmyer, M. A. Next-Generation Ultrafiltration Membranes Enabled by Block Polymers. *ACS Nano* **2020**, *14* (12), 16446−16471.
(38) Hoehn, B. D.; Kellstedt, E. A.; Hillmyer, M. A. Tough Polycyclooctene Nanoporous Membranes from Etchable Block Copolymers. *Soft Matter* **2024**, *20* (2), 437−448.
(39) Masclef, J.-B.; Acs, E. M. N.; Koehnke, J.; Prunet, J.; Schmidt, B. V. K. J. PEGose Block Poly(lactic acid) Nanoparticles for Cargo Delivery. *Macromolecules.* **2024**, *57* (13), 6013−6023.
(40) Mundel, R.; Thakur, T.; Chatterjee, M. Emerging Uses of PLA−PEG Copolymer in Cancer Drug Delivery. *3 Biotech* **2022**, *12* (2), 41.
(41) Ryner, M.; Albertsson, A.-C. Resorbable and Highly Elastic Block Copolymers from 1,5-Dioxepan-2-One and l-Lactide with Controlled Tensile Properties and Hydrophilicity. *Biomacromolecules* **2002**, *3* (3), 601−608.
(42) Wanamaker, C. L.; Bluemle, M. J.; Pitet, L. M.; O'Leary, L. E.; Tolman, W. B.; Hillmyer, M. A. Consequences of Polylactide Stereochemistry on the Properties of Polylactide-Polymenthide-Polylactide Thermoplastic Elastomers. *Biomacromolecules* **2009**, *10* (10), 2904−2911.
(43) Xiao, R. Z.; Zeng, Z. W.; Zhou, G. L.; Wang, J. J.; Li, F. Z.; Wang, A. M. Recent Advances in PEG−PLA Block Copolymer Nanoparticles. *Int. J. Nanomedicine* **2010**, *5*, 1057−1065.
(44) Cho, H.; Gao, J.; Kwon, G. S. PEG-*b*-PLA Micelles and PLGA-*b*-PEG-*b*-PLGA Sol−Gels for Drug Delivery. *J. Controlled Release* **2016**, *240*, 191−201.
(45) Oh, J. K. Polylactide (PLA)-Based Amphiphilic Block Copolymers : Synthesis, Self-Assembly, and Biomedical Applications. *Soft Matter* **2011**, *7* (11), 5096−5108.
(46) Bates, C. M.; Bates, F. S. 50th Anniversary Perspective: Block Polymers—Pure Potential. *Macromolecules* **2017**, *50* (1), 3−22.
(47) De Santis, P.; Kovacs, A. J. Molecular Conformation of Poly(S-lactic Acid). *Biopolymers* **1968**, *6* (3), 299−306.
(48) Ikada, Y.; Jamshidi, K.; Tsuji, H.; Hyon, S. H. Stereocomplex Formation between Enantiomeric Poly(Lactides). *Macromolecules* **1987**, *20*, 904−906.
(49) Tsuji, H.; Ikada, Y. Stereocomplex Formation between Enantiomeric Poly(Lactic Acid)s. XI. Mechanical Properties and Morphology of Solution-Cast Films. *Polymer* **1999**, *40* (24), 6699−6708.

(50) Tsuji, H. Poly(Lactic Acid) Stereocomplexes: A Decade of Progress. *Adv. Drug Delivery Rev.* **2016**, *107*, 97−135.
(51) Lee, S.; Kimoto, M.; Tanaka, M.; Tsuji, H.; Nishino, T. Crystal Modulus of Poly (Lactic Acid)s, and Their Stereocomplex. *Polymer* **2018**, *138*, 124−131.
(52) Li, L.; Zhong, Z.; De Jeu, W. H.; Dijkstra, P. J.; Feijen, J. Crystal Structure and Morphology of Poly(L -Lactide- *b* - D -Lactide) Diblock Copolymers. *Macromolecules* **2004**, *37* (23), 8641−8646.
(53) Liffland, S.; Kumler, M. S.; Hillmyer, M. A. High Performance Star Block Aliphatic Polyester Thermoplastic Elastomers Using PDLA-b-PLLA Stereoblock Hard Domains. *ACS Macro Lett.* **2023**, *12*, 1331.
(54) Rosen, T.; Goldberg, I.; Venditto, V.; Kol, M. Tailor-Made Stereoblock Copolymers of Poly(Lactic Acid) by a Truly Living Polymerization Catalyst. *J. Am. Chem. Soc.* **2016**, *138* (37), 12041−12044.
(55) Rosen, T.; Goldberg, I.; Navarra, W.; Venditto, V.; Kol, M. Block−Stereoblock Copolymers of Poly(ϵ -Caprolactone) and Poly(Lactic Acid). *Angew. Chem., Int. Ed.* **2018**, *57* (24), 7191−7195.
(56) Geng, X.; Liu, Z.; Zhang, C.; Zhang, X. Toward Stereo- and Sequence-Defined Block Copolymers via a Three-Site Organocatalyst. *Macromolecules* **2023**, *56* (12), 4649−4657.
(57) McKeown, P.; Davidson, M. G.; Kociok-Köhn, G.; Jones, M. D. Aluminium Salalens vs. Salans: "Initiator Design" for the Isoselective Polymerisation of Rac-Lactide. *Chem. Commun.* **2016**, *52* (68), 10431−10434.
(58) Beament, J.; Mahon, M. F.; Buchard, A.; Jones, M. D. Aluminum Complexes of Monopyrrolidine Ligands for the Controlled Ring-Opening Polymerization of Lactide. *Organometallics* **2018**, *37* (11), 1719−1724.
(59) Zaky, M. S.; Wirotius, A.-L.; Coulembier, O.; Guichard, G.; Taton, D. Reaching High Stereoselectivity and Activity in Organocatalyzed Ring-Opening Polymerization of Racemic Lactide by the Combined Use of a Chiral (Thio)Urea and a *N* -Heterocyclic Carbene. *ACS Macro Lett.* **2022**, *11* (9), 1148−1155.
(60) Zaky, M. S.; Guichard, G.; Taton, D. Structural Effect of Organic Catalytic Pairs Based on Chiral Amino(Thio)Ureas and Phosphazene Bases for the Isoselective Ring-Opening Polymerization of Racemic Lactide. *Macromolecules* **2023**, *56* (10), 3607−3616.
(61) Morodo, R.; Dumas, D. M.; Zhang, J.; Lui, K. H.; Hurst, P. J.; Bosio, R.; Campos, L. M.; Park, N. H.; Waymouth, R. M.; Hedrick, J. L. Ring-Opening Polymerization of Cyclic Esters and Carbonates with (Thio)Urea/Cyclopropenimine Organocatalytic Systems. *ACS Macro Lett.* **2024**, 181−188.
(62) Refaa, Z.; Boutaous, M.; Siginer, D. A. PLA Crystallization Kinetics and Morphology Development. *Int. Polym. Process.* **2018**, *33* (3), 336−344.
(63) De Santis, F.; Volpe, V.; Pantani, R. Effect of Molding Conditions on Crystallization Kinetics and Mechanical Properties of Poly(Lactic Acid). *Polym. Eng. Sci.* **2017**, *57* (3), 306−311.
(64) Saeidlou, S.; Huneault, M. A.; Li, H.; Park, C. B. Poly(Lactic Acid) Crystallization. *Prog. Polym. Sci.* **2012**, *37* (12), 1657−1677.
(65) Kurcok, P.; Penczek, J.; Franek, J.; Jedlinski, Z. Anionic Polymerization of Lactones. 14. Anionic Block Copolymerization of δ-Valerolactone and L-Lactide Initiated with Potassium Methoxide. *Macromolecules* **1992**, *25* (9), 2285−2289.
(66) Schmidt, S. C.; Hillmyer, M. A. Synthesis and Characterization of Model Polyisoprene−Polylactide Diblock Copolymers. *Macromolecules* **1999**, *32* (15), 4794−4801.
(67) Frick, E. M.; Hillmyer, M. A. Synthesis and Characterization of Polylactide-Block-Polyisoprene-Block-Polylactide Triblock Copolymers: New Thermoplastic Elastomers Containing Biodegradable Segments. *Macromol. Rapid Commun.* **2000**, *21* (18), 1317−1322.
(68) Bachari, A.; Belorgey, G.; Helary, G.; Sauvet, G. Synthesis and Characterization of Multiblock Copolymers Poly [Poly(L-Lactide)-Block-Polydimethylsiloxane]. *Macromol. Chem. Phys.* **1995**, *196*, 411−428.
(69) Sipos, L.; Zsuga, M.; Deák, G. Synthesis of Poly(L-Lactide)-Block-Polyisobutylene-Block-Poly(L-Lactide), a New Biodegradable Thermoplastic Elastomer. *Macromol. Rapid Commun.* **1995**, *16* (12), 935−940.
(70) Albanese, K. R.; Blankenship, J. R.; Quah, T.; Zhang, A.; Delaney, K. T.; Fredrickson, G. H.; Bates, C. M.; Hawker, C. J. Improved Elastic Recovery from ABC Triblock Terpolymers. *ACS Polym. Au* **2023**, *3*, 376.
(71) Yildirim, I.; Sungur, P.; Crecelius-Vitz, A. C.; Yildirim, T.; Kalden, D.; Hoeppener, S.; Westerhausen, M.; Weber, C.; Schubert, U. S. One-Pot Synthesis of PLA-b-PHEA via Sequential ROP and RAFT Polymerizations. *Polym. Chem.* **2017**, *8* (39), 6086−6098.
(72) Si, G.; Li, C.; Chen, M.; Chen, C. Polymer Multi-Block and Multi-Block $^{+}$ Strategies for the Upcycling of Mixed Polyolefins and Other Plastics. *Angew. Chem., Int. Ed.* **2023**, *62* (49), No. e202311733.
(73) Jabbar, R.; Graffe, A.; Lessard, B.; Marić, M. Nitroxide-mediated Synthesis of Styrenic-based Segmented and Tapered Block Copolymers Using Poly(Lactide)-functionalized TEMPO Macromediators. *J. Appl. Polym. Sci.* **2008**, *109* (5), 3185−3195.
(74) Bolton, J.; Rzayev, J. Synthesis and Melt Self-Assembly of PS−PMMA−PLA Triblock Bottlebrush Copolymers. *Macromolecules* **2014**, *47* (9), 2864−2874.
(75) Romain, C.; Williams, C. K. Chemoselective Polymerization Control: From Mixed-Monomer Feedstock to Copolymers. *Angew. Chem., Int. Ed.* **2014**, *53* (6), 1607−1610.
(76) Deacy, A. C.; Gregory, G. L.; Sulley, G. S.; Chen, T. T. D.; Williams, C. K. Sequence Control from Mixtures: Switchable Polymerization Catalysis and Future Materials Applications. *J. Am. Chem. Soc.* **2021**, *143* (27), 10021−10040.
(77) Stößer, T.; Mulryan, D.; Williams, C. K. Switch Catalysis To Deliver Multi-Block Polyesters from Mixtures of Propene Oxide, Lactide, and Phthalic Anhydride. *Angew. Chem., Int. Ed.* **2018**, *57* (51), 16893−16897.
(78) Wang, X.; Thevenon, A.; Brosmer, J. L.; Yu, I.; Khan, S. I.; Mehrkhodavandi, P.; Diaconescu, P. L. Redox Control of Group 4 Metal Ring-Opening Polymerization Activity toward L -Lactide and ϵ-Caprolactone. *J. Am. Chem. Soc.* **2014**, *136* (32), 11264−11267.
(79) Liu, J.; Blosch, S. E.; Volokhova, A. S.; Crater, E. R.; Gallin, C. F.; Moore, R. B.; Matson, J. B.; Byers, J. A. Using Redox-Switchable Polymerization Catalysis to Synthesize a Chemically Recyclable Thermoplastic Elastomer. *Angew. Chem., Int. Ed.* **2024**, *63* (6), No. e202317699.
(80) Biernesser, A. B.; Delle Chiaie, K. R.; Curley, J. B.; Byers, J. A. Block Copolymerization of Lactide and an Epoxide Facilitated by a Redox Switchable Iron-Based Catalyst. *Angew. Chem., Int. Ed.* **2016**, *55* (17), 5251−5254.
(81) Biernesser, A. B.; Li, B.; Byers, J. A. Redox-Controlled Polymerization of Lactide Catalyzed by Bis(Imino)Pyridine Iron Bis(Alkoxide) Complexes. *J. Am. Chem. Soc.* **2013**, *135* (44), 16553−16560.
(82) Hong, S.-J.; Jeong, H.; Yuk, J. S.; Park, M.; Kim, G.; Kim, Y.-W.; Shin, J. Semicrystalline-Glassy Multiblock Copolymers via Mechanochemical Synthesis toward Tough Poly(Lactide). *ACS Sustain. Chem. Eng.* **2022**, *10* (44), 14523−14538.
(83) Jikei, M.; Takeyama, Y.; Yamadoi, Y.; Shinbo, N.; Matsumoto, K.; Motokawa, M.; Ishibashi, K.; Yamamoto, F. Synthesis and Properties of Poly(L-Lactide)-Poly(ε-Caprolactone) Multiblock Copolymers by the Self-Polycondensation of Diblock Macromonomers. *Polym. J.* **2015**, *47* (10), 657−665.
(84) Liffland, S.; Hillmyer, M. A. Enhanced Mechanical Properties of Aliphatic Polyester Thermoplastic Elastomers through Star Block Architectures. *Macromolecules* **2021**, *54* (20), 9327−9340.
(85) Michalski, A.; Brzezinski, M.; Lapienis, G.; Biela, T. Star-Shaped and Branched Polylactides: Synthesis, Characterization, and Properties. *Prog. Polym. Sci.* **2019**, *89*, 159−212.
(86) Lee, S.; Lee, K.; Jang, J.; Choung, J. S.; Choi, W. J.; Kim, G.-J.; Kim, Y.-W.; Shin, J. Sustainable Poly(ε-Decalactone)−poly(l-Lactide) Multiarm Star Copolymer Architectures for Thermoplastic Elastomers with Fixed Molar Mass and Block Ratio. *Polymer* **2017**, *112*, 306−317.

https://doi.org/10.1021/acs.biomac.5c00161
Biomacromolecules 2025, 26, 2761−2783

(87) Liu, M.; Blankenship, J. R.; Levi, A. E.; Fu, Q.; Hudson, Z. M.; Bates, C. M. Miktoarm Star Polymers: Synthesis and Applications. *Chem. Mater.* **2022**, *34* (14), 6188−6209.
(88) Levi, A. E.; Fu, L.; Lequieu, J.; Horne, J. D.; Blankenship, J.; Mukherjee, S.; Zhang, T.; Fredrickson, G. H.; Gutekunst, W. R.; Bates, C. M. Efficient Synthesis of Asymmetric Miktoarm Star Polymers. *Macromolecules* **2020**, *53* (2), 702−710.
(89) Blankenship, J. R.; Levi, A. E.; Goldfeld, D. J.; Self, J. L.; Alizadeh, N.; Chen, D.; Fredrickson, G. H.; Bates, C. M. Asymmetric Miktoarm Star Polymers as Polyester Thermoplastic Elastomers. *Macromolecules* **2022**, *55* (12), 4929−4936.
(90) Roovers, J.; Toporowski, P. M. Preparation and Characterization of H-Shaped Polystyrene. *Macromolecules* **1981**, *14* (5), 1174−1178.
(91) Zografos, A.; Maines, E. M.; Hassler, J. F.; Bates, F. S.; Hillmyer, M. A. Preparation and Characterization of H-Shaped Polylactide. *ACS Macro Lett.* **2024**, *13* (6), 695−702.
(92) Meier-Merziger, M.; Imschweiler, J.; Hartmann, F.; Niebuur, B.; Kraus, T.; Gallei, M.; Frey, H. Bifunctional Carbanionic Synthesis of Fully Bio-Based Triblock Structures Derived from β -Farnesene and LL -Dilactide: Thermoplastic Elastomers. *Angew. Chem., Int. Ed.* **2023**, *62* (42), No. e202310519.
(93) Meier-Merziger, M.; Fickenscher, M.; Hartmann, F.; Kuttich, B.; Kraus, T.; Gallei, M.; Frey, H. Synthesis of Phase-Separated Super-H-Shaped Triblock Architectures: Poly(L -Lactide) Grafted from Telechelic Polyisoprene. *Polym. Chem.* **2023**, *14* (23), 2820−2828.
(94) Lodge, T. P.; Hiemenz, P. C. *Polymer Chemistry*, 3rd ed.; CRC Press: Boca Raton, FL, 2020.
(95) Matsen, M. W.; Bates, F. S. Unifying Weak- and Strong-Segregation Block Copolymer Theories. *Macromolecules* **1996**, *29* (4), 1091−1098.
(96) Matsen, M. W.; Thompson, R. B. Equilibrium Behavior of Symmetric ABA Triblock Copolymer Melts. *J. Chem. Phys.* **1999**, *111* (15), 7139−7146.
(97) Lai, W.-C.; Liau, W.-B.; Lin, T.-T. The Effect of End Groups of PEG on the Crystallization Behaviors of Binary Crystalline Polymer Blends PEG/PLLA. *Polymer* **2004**, *45* (9), 3073−3080.
(98) Hampu, N.; Hillmyer, M. A. Molecular Engineering of Nanostructures in Disordered Block Polymers. *ACS Macro Lett.* **2020**, *9* (3), 382−388.
(99) Antoine, S.; Geng, Z.; Zofchak, E. S.; Chwatko, M.; Fredrickson, G. H.; Ganesan, V.; Hawker, C. J.; Lynd, N. A.; Segalman, R. A. Non-Intuitive Trends in Flory−Huggins Interaction Parameters in Polyether-Based Polymers. *Macromolecules* **2021**, *54* (14), 6670−6677.
(100) Schneiderman, D. K.; Hill, E. M.; Martello, M. T.; Hillmyer, M. A. Poly(Lactide)-Block-Poly(ϵ-Caprolactone-Co-ϵ-Decalactone)-Block-Poly(Lactide) Copolymer Elastomers. *Polym. Chem.* **2015**, *6* (19), 3641−3651.
(101) Watts, A.; Kurokawa, N.; Hillmyer, M. A. Strong, Resilient, and Sustainable Aliphatic Polyester Thermoplastic Elastomers. *Biomacromolecules* **2017**, *18* (6), 1845−1854.
(102) Martello, M. T.; Hillmyer, M. A. Polylactide−Poly(6-Methyl-ϵ-Caprolactone)−Polylactide Thermoplastic Elastomers. *Macromolecules* **2011**, *44* (21), 8537−8545.
(103) Martello, M. T.; Schneiderman, D. K.; Hillmyer, M. A. Synthesis and Melt Processing of Sustainable Poly(ϵ-Decalactone)-Block-Poly(Lactide) Multiblock Thermoplastic Elastomers. *ACS Sustain. Chem. Eng.* **2014**, *2* (11), 2519−2526.
(104) Lee, I.; Panthani, T. R.; Bates, F. S. Sustainable Poly(Lactide-b-Butadiene) Multiblock Copolymers with Enhanced Mechanical Properties. *Macromolecules* **2013**, *46* (18), 7387−7398.
(105) Lee, S.; Gillard, T. M.; Bates, F. S. Fluctuations, Order, and Disorder in Short Diblock Copolymers. *AIChE J.* **2013**, *59* (9), 3502−3513.
(106) Yao, L.; Oquendo, L. E.; Schulze, M. W.; Lewis, R. M. I.; Gladfelter, W. L.; Hillmyer, M. A. Poly(Cyclohexylethylene)-Block-Poly(Lactide) Oligomers for Ultrasmall Nanopatterning Using Atomic Layer Deposition. *ACS Appl. Mater. Interfaces* **2016**, *8* (11), 7431−7439.
(107) Cushen, J. D.; Bates, C. M.; Rausch, E. L.; Dean, L. M.; Zhou, S. X.; Willson, C. G.; Ellison, C. J. Thin Film Self-Assembly of Poly(Trimethylsilylstyrene-b-d,l-Lactide) with Sub-10 Nm Domains. *Macromolecules* **2012**, *45* (21), 8722−8728.
(108) Anderson, K. S.; Lim, S. H.; Hillmyer, M. A. Toughening of Polylactide by Melt Blending with Linear Low-Density Polyethylene. *J. Appl. Polym. Sci.* **2003**, *89* (14), 3757−3768.
(109) Wanamaker, C. L.; O'Leary, L. E.; Lynd, N. A.; Hillmyer, M. A.; Tolman, W. B. Renewable-Resource Thermoplastic Elastomers Based on Polylactide and Polymenthide. *Biomacromolecules* **2007**, *8* (11), 3634−3640.
(110) Schmidt, S. C.; Hillmyer, M. A. Morphological Behavior of Model Poly(Ethylene-Alt-Propylene)-b-Polylactide Diblock Copolymers. *J. Polym. Sci., Part B: Polym. Phys.* **2002**, *40* (20), 2364−2376.
(111) Rodwogin, M. D.; Spanjers, C. S.; Leighton, C.; Hillmyer, M. A. Polylactide−Poly(Dimethylsiloxane)−Polylactide Triblock Copolymers as Multifunctional Materials for Nanolithographic Applications. *ACS Nano* **2010**, *4* (2), 725−732.
(112) Lynd, N. A.; Hillmyer, M. A. Influence of Polydispersity on the Self-Assembly of Diblock Copolymers. *Macromolecules* **2005**, *38* (21), 8803−8810.
(113) Sides, S. W.; Fredrickson, G. H. Continuous Polydispersity in a Self-Consistent Field Theory for Diblock Copolymers. *J. Chem. Phys.* **2004**, *121* (10), 4974−4986.
(114) Schmitt, A. K.; Mahanthappa, M. K. Characteristics of Lamellar Mesophases in Strongly Segregated Broad Dispersity ABA Triblock Copolymers. *Macromolecules* **2014**, *47* (13), 4346−4356.
(115) Schmitt, A. K.; Mahanthappa, M. K. Order and Disorder in High χ/Low N, Broad Dispersity ABA Triblock Polymers. *Macromolecules* **2017**, *50* (17), 6779−6787.
(116) Mayes, A. M.; Olvera de la Cruz, M. Microphase Separation in Multiblock Copolymer Melts. *J. Chem. Phys.* **1989**, *91* (11), 7228−7235.
(117) Ma, Z.; Liu, Z.; Zheng, T.; Gan, Z.; Tan, R.; Dong, X.-H. Discrete Miktoarm Star Block Copolymers with Tailored Molecular Architecture. *ACS Polym. Au* **2023**, *3* (6), 457−465.
(118) Matsen, M. W. Effect of Architecture on the Phase Behavior of AB-Type Block Copolymer Melts. *Macromolecules* **2012**, *45* (4), 2161−2165.
(119) Li, C.; Dong, Q.; Li, W. Largely Tunable Asymmetry of Phase Diagrams of A(AB)n Miktoarm Star Copolymer. *Macromolecules* **2020**, *53* (24), 10907−10917.
(120) Anderson, K. S.; Hillmyer, M. A. Melt Chain Dimensions of Polylactide. *Macromolecules* **2004**, *37* (5), 1857−1862.
(121) Pitet, L. M.; Chamberlain, B. M.; Hauser, A. W.; Hillmyer, M. A. Dispersity and Architecture Driven Self-Assembly and Confined Crystallization of Symmetric Branched Block Copolymers. *Polym. Chem.* **2019**, *10* (39), 5385−5395.
(122) Bailey, T. *Morphological Behavior Spanning the Symmetric AB and ABC Block Copolymer States*. Ph.D. Dissertation, University of Minnesota, Department of Chemical Engineering and Material Science, Minneapolis, MN, 2001.
(123) Cui, S.; Murphy, E. A.; Zhang, W.; Zografos, A.; Shen, L.; Bates, F. S.; Lodge, T. P. Cylinders-in-Undulating-Lamellae Morphology from ABC Bottlebrush Block Terpolymers. *J. Am. Chem. Soc.* **2024**, *146* (10), 6796−6805.
(124) Zhou, J.; Jiang, Z.; Wang, Z.; Zhang, J.; Li, J.; Li, Y.; Zhang, J.; Chen, P.; Gu, Q. Synthesis and Characterization of Triblock Copolymer PLA-b-PBT-b-PLA and Its Effect on the Crystallization of PLA. *RSC Adv.* **2013**, *3* (40), 18464−18473.
(125) Maillard, D.; Prud'homme, R. E. Chirality Information Transfer in Polylactides: From Main-Chain Chirality to Lamella Curvature. *Macromolecules* **2006**, *39* (13), 4272−4275.
(126) Chao, C.-C.; Chen, C.-K.; Chiang, Y.-W.; Ho, R.-M. Banded Spherulites in PS−PLLA Chiral Block Copolymers. *Macromolecules* **2008**, *41* (11), 3949−3956.

https://doi.org/10.1021/acs.biomac.5c00161
Biomacromolecules 2025, 26, 2761−2783

(127) Cornelissen, J. J. L. M.; Fischer, M.; Sommerdijk, N. A. J. M.; Nolte, R. J. M. Helical Superstructures from Charged Poly(Styrene)-Poly(Isocyanodipeptide) Block Copolymers. *Science* **1998**, *280* (5368), 1427−1430.
(128) Ho, R.-M.; Chiang, Y.-W.; Tsai, C.-C.; Lin, C.-C.; Ko, B.-T.; Huang, B.-H. Three-Dimensionally Packed Nanohelical Phase in Chiral Block Copolymers. *J. Am. Chem. Soc.* **2004**, *126* (9), 2704−2705.
(129) Ho, R.-M.; Chiang, Y.-W.; Chen, C.-K.; Wang, H.-W.; Hasegawa, H.; Akasaka, S.; Thomas, E. L.; Burger, C.; Hsiao, B. S. Block Copolymers with a Twist. *J. Am. Chem. Soc.* **2009**, *131* (51), 18533−18542.
(130) Ho, R.-M.; Li, M.-C.; Lin, S.-C.; Wang, H.-F.; Lee, Y.-D.; Hasegawa, H.; Thomas, E. L. Transfer of Chirality from Molecule to Phase in Self-Assembled Chiral Block Copolymers. *J. Am. Chem. Soc.* **2012**, *134* (26), 10974−10986.
(131) Yuan, J.; Chiu, P.-T.; Liu, X.; Zhou, J.; Wang, Y.; Ho, R.-M.; Wen, T. Cross-Domain Chirality Transfer in Self-Assembly of Chiral Block Copolymers. *Angew. Chem., Int. Ed.* **2024**, *63* (7), No. e202317102.
(132) Wang, H.-F.; Chiu, P.-T.; Yang, C.-Y.; Xie, Z.-H.; Hung, Y.-C.; Lee, J.-Y.; Tsai, J.-C.; Prasad, I.; Jinnai, H.; Thomas, E. L.; Ho, R.-M. Networks with Controlled Chirality via Self-Assembly of Chiral Triblock Terpolymers. *Sci. Adv.* **2020**, *6* (42), No. eabc3644.
(133) Creton, C. Pressure-Sensitive Adhesives: An Introductory Course. *MRS Bull.* **2003**, *28* (6), 434−439.
(134) Kraus, G.; Jones, F. B.; Marrs, O. L.; Rollmann, K. W. Morphology and Viscoelastic Behavior of Styrene-Diene Block Copolymers in Pressure Sensitive Adhesives. *J. Adhes.* **1976**, *8* (3), 235−258.
(135) Shin, J.; Martello, M. T.; Shrestha, M.; Wissinger, J. E.; Tolman, W. B.; Hillmyer, M. A. Pressure-Sensitive Adhesives from Renewable Triblock Copolymers. *Macromolecules* **2011**, *44* (1), 87−94.
(136) Cathie, K. The Effect of Packaging Adhesives on Wastepaper Recycling—a Review. *Int. J. Adhes. Adhes.* **1994**, *14* (1), 63−67.
(137) Lee, S.; Lee, K.; Kim, Y.-W.; Shin, J. Preparation and Characterization of a Renewable Pressure-Sensitive Adhesive System Derived from ε-Decalactone, l-Lactide, Epoxidized Soybean Oil, and Rosin Ester. *ACS Sustain. Chem. Eng.* **2015**, *3* (9), 2309−2320.
(138) Ewert, T. R.; Mannion, A. M.; Coughlin, M. L.; Macosko, C. W.; Bates, F. S. Influence of Rheology on Renewable Pressure-Sensitive Adhesives from a Triblock Copolymer. *J. Rheol.* **2018**, *62* (1), 161−170.
(139) Chang, E. P. Viscoelastic Windows of Pressure-Sensitive Adhesives. *J. Adhes.* **1991**, *34* (1−4), 189−200.
(140) Xu, C.; Wang, L.; Liu, Y.; Niu, H.; Shen, Y.; Li, Z. Rapid and Controlled Ring-Opening (Co)Polymerization of Bio-Sourced Alkyl-δ-Lactones To Produce Recyclable (Co)Polyesters and Their Application as Pressure-Sensitive Adhesives. *Macromolecules* **2023**, *56* (15), 6117−6125.
(141) Kim, H. J.; Jin, K.; Shim, J.; Dean, W.; Hillmyer, M. A.; Ellison, C. J. Sustainable Triblock Copolymers as Tunable and Degradable Pressure Sensitive Adhesives. *ACS Sustain. Chem. Eng.* **2020**, *8* (32), 12036−12044.
(142) Liang, S.; Krajovic, D. M.; Hoehn, B. D.; Ellison, C. J.; Hillmyer, M. A. Engineering Aliphatic Polyester Triblock Copolymer-Tackifier Blends for Hydrolytically Degradable Pressure Sensitive Adhesives. *ACS Appl. Polym. Mater.* **2025**, *7* (3), 1411−1420.
(143) *Thermoplastic Elastomers*, 3rd ed.; Kricheldorf, H. R., Quirk, R. P., Holden, G., Eds.; Hanser Gardner Publications: Cincinnati, 2004.
(144) *Thermoplastic Elastomers Market Size, Share & Trends Analysis Report By Application (Automotive, Industrial, Medical), By Material (Poly Styrenes, Poly Olefins), By Region, And Segment Forecasts, 2024 - 2030*; 978-1-68038-478-9; Grand View Research. https://www.grandviewresearch.com/industry-analysis/thermoplastic-elastomers-market (accessed 2024-12-16).
(145) Zhang, S.; Hou, Z.; Gonsalves, K. E. Copolymer Synthesis of Poly(L-Lactide-b-DMS-L-Lactide) via the Ring Opening Polymerization of L-Lactide in the Presence of α,ω-Hydroxylpropyl-Terminated PDMS Macroinitiator. *J. Polym. Sci. Part Polym. Chem.* **1996**, *34* (13), 2737−2742.
(146) Gregory, G. L.; Sulley, G. S.; Carrodeguas, L. P.; Chen, T. T. D.; Santmarti, A.; Terrill, N. J.; Lee, K.-Y.; Williams, C. K. Triblock Polyester Thermoplastic Elastomers with Semi-Aromatic Polymer End Blocks by Ring-Opening Copolymerization. *Chem. Sci.* **2020**, *11* (25), 6567−6581.
(147) Fournier, L.; Rivera Mirabal, D. M.; Hillmyer, M. A. Toward Sustainable Elastomers from the Grafting-Through Polymerization of Lactone-Containing Polyester Macromonomers. *Macromolecules* **2022**, *55* (3), 1003−1014.
(148) De Hoe, G. X.; Zumstein, M. T.; Tiegs, B. J.; Brutman, J. P.; McNeill, K.; Sander, M.; Coates, G. W.; Hillmyer, M. A. Sustainable Polyester Elastomers from Lactones: Synthesis, Properties, and Enzymatic Hydrolyzability. *J. Am. Chem. Soc.* **2018**, *140* (3), 963−973.
(149) Batiste, D. C.; Meyersohn, M. S.; Watts, A.; Hillmyer, M. A. Efficient Polymerization of Methyl-ε-Caprolactone Mixtures To Access Sustainable Aliphatic Polyesters. *Macromolecules* **2020**, *53* (5), 1795−1808.
(150) Reisman, L.; Siehr, A.; Horn, J.; Batiste, D. C.; Kim, H. J.; De Hoe, G. X.; Ellison, C. J.; Shen, W.; White, E. M.; Hillmyer, M. A. Respirometry and Cell Viability Studies for Sustainable Polyesters and Their Hydrolysis Products. *ACS Sustain. Chem. Eng.* **2021**, *9* (7), 2736−2744.
(151) Liffland, S.; Kumler, M.; Hillmyer, M. A. High Performance Star Block Aliphatic Polyester Thermoplastic Elastomers Using PDLA-b-PLLA Stereoblock Hard Domains. *ACS Macro Letters* **2023**, *12* (10, Suppl. 1), 1331−1338.
(152) Xiong, M.; Schneiderman, D. K.; Bates, F. S.; Hillmyer, M. A.; Zhang, K. Scalable Production of Mechanically Tunable Block Polymers from Sugar. *Proc. Natl. Acad. Sci. U. S. A.* **2014**, *111* (23), 8357−8362.
(153) Zhang, J.; Li, T.; Mannion, A. M.; Schneiderman, D. K.; Hillmyer, M. A.; Bates, F. S. Tough and Sustainable Graft Block Copolymer Thermoplastics. *ACS Macro Lett.* **2016**, *5* (3), 407−412.
(154) Siehr, A.; Flory, C.; Callaway, T.; Schumacher, R. J.; Siegel, R. A.; Shen, W. Implantable and Degradable Thermoplastic Elastomer. *ACS Biomater. Sci. Eng.* **2021**, *7* (12), 5598−5610.
(155) Schüttner, S.; Gardiner, C.; Petrov, F. S.; Fotaras, N.; Preis, J.; Floudas, G.; Frey, H. Biobased Thermoplastic Elastomers Derived from Citronellyl Glycidyl Ether, CO_2, and Polylactide. *Macromolecules* **2023**, *56* (20), 8247−8259.
(156) Yuk, J. S.; Mo, E.; Kim, S.; Jeong, H.; Gwon, H.; Kim, N.-K.; Kim, Y.-W.; Shin, J. Thermoplastic Superelastomers Based on Poly(Isobutylene)- *Graft* -Poly(L -Lactide) Copolymers: Enhanced Thermal Stability, Tunable Tensile Strength, and Gas Barrier Property. *Macromolecules* **2020**, *53* (7), 2503−2515.
(157) Nakayama, Y.; Aihara, K.; Yamanishi, H.; Fukuoka, H.; Tanaka, R.; Cai, Z.; Shiono, T. Synthesis of Biodegradable Thermoplastic Elastomers from ε -caprolactone and Lactide. *J. Polym. Sci. Part Polym. Chem.* **2015**, *53* (3), 489−495.
(158) Zhao, W.; Li, C.; Yang, X.; He, J.; Pang, X.; Zhang, Y.; Men, Y.; Chen, X. One-Pot Synthesis of Supertough, Sustainable Polyester Thermoplastic Elastomers Using Block-Like, Gradient Copolymer as Soft Midblock. *CCS Chem.* **2022**, *4* (4), 1263−1272.
(159) Huang, W.; Zhu, N.; Liu, Y.; Wang, J.; Zhong, J.; Sun, Q.; Sun, T.; Hu, X.; Fang, Z.; Guo, K. A Novel Microfluidic Enzyme-Organocatalysis Combination Strategy for Ring-Opening Copolymerizations of Lactone, Lactide and Cyclic Carbonate. *Chem. Eng. J.* **2019**, *356*, 592−597.
(160) Ji, C. L.; Jie, S.; Li, B. Ring-Opening Copolymerization of L-Lactide and δ-Valerolactone Catalyzed by Benzoxazolyl Urea Catalyst/MTBD. *Acta Polym. Sin.* **2022**, *53* (5), 488−496.
(161) Wang, X.; Liu, J.; Xu, S.; Xu, J.; Pan, X.; Liu, J.; Cui, S.; Li, Z.; Guo, K. Traceless Switch Organocatalysis Enables Multiblock Ring-Opening Copolymerizations of Lactones, Carbonates, and Lactides:

https://doi.org/10.1021/acs.biomac.5c00161
Biomacromolecules 2025, 26, 2761−2783

By a One plus One Approach in One Pot. *Polym. Chem.* **2016**, *7* (41), 6297−6308.
(162) Zhu, Y.; Gao, L.; Li, Z.; Liu, B.; Zhang, Z.; Tong, H.; Qu, Y.; Quan, Y.; Zou, X.; Guo, K. Merging of Cationic RAFT and Radical RAFT Polymerizations with Ring-Opening Polymerizations for the Synthesis of Asymmetric ABCD Type Tetrablock Copolymers in One Pot. *Polym. Chem.* **2021**, *12* (34), 4974−4985.
(163) Zhu, Y.; Hu, Y.; Li, Z.; Liu, B.; Qu, Y.; Zhang, Z.; Guo, T.; Li, Y.; Gao, L.; Guo, K. A Genuine H-Bond Donor and Lewis Base Amine Cocatalyst in Ring-Opening Polymerizations. *Eur. Polym. J.* **2021**, *143*, No. 110184.
(164) Anderson, R. J.; Fine, R. L.; Rapagnani, R. M.; Tonks, I. A. Ring-Opening Copolymerizations of a CO2-Derived δ-Valerolactone with ε-Caprolactone and l-Lactide. *Macromolecules* **2024**, *57* (13), 6248−6254.
(165) Feng, X.; Geng, X.; Zhang, C.; Zhang, X. Chain Shuttle between Dual Sites of a Monomolecular Organocatalyst Enables Controlled Ring-Opening Copolymerization. *Macromolecules* **2024**, *57* (17), 8401−8408.
(166) Liang, J.; Yang, J. Organocatalytic Regulation from Salicylic O-Carboxyanhydrides and l-Lactide Mixtures to Sequence-Defined Copolymers. *Macromolecules* **2024**, *57* (19), 9265−9274.
(167) Li, Y.; Kou, X.; Wang, X.; Xia, L.; Li, Z. A One-Pot Approach towards Polycarbonate-b-Polyester Block Copolymers via Chemoselective Polymerization Catalyzed by a One-Component Phosphonium Borane Lewis Pair. *Polym. Chem.* **2024**, *15* (24), 2476−2481.
(168) Fu, X.; Lin, X.; Wang, M.; Ding, Z.; Ma, G.; Wang, B.; Li, Y. One-Step Synthesis of Sequence-Defined Polypeptide-Block-Polyester by Lewis Pair-Catalyzed Chemo-Selective Copolymerization. *Macromolecules* **2024**, *57* (12), 5691−5701.
(169) Theryo, G.; Jing, F.; Pitet, L. M.; Hillmyer, M. A. Tough Polylactide Graft Copolymers. *Macromolecules* **2010**, *43* (18), 7394−7397.
(170) Haugan, I. N.; Lee, B.; Maher, M. J.; Zografos, A.; Schibur, H. J.; Jones, S. D.; Hillmyer, M. A.; Bates, F. S. Physical Aging of Polylactide-Based Graft Block Polymers. *Macromolecules* **2019**, *52* (22), 8878−8894.
(171) Mannion, A. M.; Bates, F. S.; Macosko, C. W. Synthesis and Rheology of Branched Multiblock Polymers Based on Polylactide. *Macromolecules* **2016**, *49* (12), 4587−4598.
(172) Panthani, T. R.; Bates, F. S. Crystallization and Mechanical Properties of Poly(l-Lactide)-Based Rubbery/Semicrystalline Multiblock Copolymers. *Macromolecules* **2015**, *48* (13), 4529−4540.
(173) Krajovic, D. M.; Haugstad, G.; Hillmyer, M. A. Crystallinity-Independent Toughness in Renewable Poly(l-Lactide) Triblock Plastics. *Macromolecules* **2024**, *57* (6), 2818−2834.
(174) Zhang, J.; Schneiderman, D. K.; Li, T.; Hillmyer, M. A.; Bates, F. S. Design of Graft Block Polymer Thermoplastics. *Macromolecules* **2016**, *49* (23), 9108−9118.
(175) Mulchandani, N.; Masutani, K.; Kumar, S.; Yamane, H.; Sakurai, S.; Kimura, Y.; Katiyar, V. Toughened PLA-b-PCL-b-PLA Triblock Copolymer Based Biomaterials: Effect of Self-Assembled Nanostructure and Stereocomplexation on the Mechanical Properties. *Polym. Chem.* **2021**, *12* (26), 3806−3824.
(176) Dong, B.; Xu, G.; Yang, R.; Guo, X.; Wang, Q. Preparation of Block Copolymers by a Sequential Transesterification Strategy: A Feasible Route for Upcycling End-of-Life Polyester Plastics to Elastomers. *Macromolecules* **2023**, *56* (24), 10143−10152.
(177) Higgins, J. S.; Lipson, J. E. G.; White, R. P. A Simple Approach to Polymer Mixture Miscibility. *Philos. Trans. R. Soc. Math. Phys. Eng. Sci.* **2010**, *368* (1914), 1009−1025.
(178) Self, J. L.; Zervoudakis, A. J.; Peng, X.; Lenart, W. R.; Macosko, C. W.; Ellison, C. J. Linear, Graft, and Beyond: Multiblock Copolymers as Next-Generation Compatibilizers. *JACS Au* **2022**, *2* (2), 310−321.
(179) Anderson, K. S.; Hillmyer, M. A. The Influence of Block Copolymer Microstructure on the Toughness of Compatibilized Polylactide/Polyethylene Blends. *Polymer* **2004**, *45* (26), 8809−8823.
(180) Thurber, C. M.; Xu, Y.; Myers, J. C.; Lodge, T. P.; Macosko, C. W. Accelerating Reactive Compatibilization of PE/PLA Blends by an Interfacially Localized Catalyst. *ACS Macro Lett.* **2015**, *4* (1), 30−33.
(181) Hong, S.-J.; Kim, G. R.; Kim, N.-K.; Shin, J.; Kim, Y.-W. Poly(Amide11)-Incorporated Block Copolymers as Compatibilizers to Toughen a Poly(Lactide)/Polyamide 11 Blend. *ACS Appl. Polym. Mater.* **2024**, *6* (2), 1224−1235.
(182) Tan, B. H.; Muiruri, J. K.; Li, Z.; He, C. Recent Progress in Using Stereocomplexation for Enhancement of Thermal and Mechanical Property of Polylactide. *ACS Sustain. Chem. Eng.* **2016**, *4* (10), 5370−5391.
(183) Wu, B.; Zeng, Q.; Niu, D.; Yang, W.; Dong, W.; Chen, M.; Ma, P. Design of Supertoughened and Heat-Resistant PLLA/Elastomer Blends by Controlling the Distribution of Stereocomplex Crystallites and the Morphology. *Macromolecules* **2019**, *52* (3), 1092−1103.
(184) Chen, J.; Rong, C.; Lin, T.; Chen, Y.; Wu, J.; You, J.; Wang, H.; Li, Y. Stable Co-Continuous PLA/PBAT Blends Compatibilized by Interfacial Stereocomplex Crystallites: Toward Full Biodegradable Polymer Blends with Simultaneously Enhanced Mechanical Properties and Crystallization Rates. *Macromolecules* **2021**, *54* (6), 2852−2861.
(185) Chen, X.; Li, C.; Ding, Y.; Li, Y.; Li, J.; Sun, L.; Wei, J.; Wei, X.; Wang, H.; Zhang, K.; Pan, L.; Li, Y. Fully Bio-Based and Supertough PLA Blends via a Novel Interlocking Strategy Combining Strong Dipolar Interactions and Stereocomplexation. *Macromolecules* **2022**, *55* (13), 5864−5878.
(186) Li, C.; Meng, X.; Gong, W.; Chen, S.; Wen, W.; Xin, Z. Super Toughened PLLA/PBAT Blends with Modified Phase Interface via Constructing Cocontinuous Structure with the Aid of Stereocomplex Crystallites Toward Preparation of a Fully Degradable Material. *Ind. Eng. Chem. Res.* **2023**, *62* (50), 21682−21692.
(187) Paul, D. R.; Barlow, J. W. Polymer Blends. *J. Macromol. Sci. Part C* **1980**, *18* (1), 109−168.
(188) Lee, B.; Maher, M. J.; Schibur, H. J.; Hillmyer, M. A.; Bates, F. S. Toughening Polylactide with Graft-Block Polymers. *ACS Appl. Polym. Mater.* **2022**, *4* (5), 3408−3416.
(189) Wang, Z.; Zhao, Y.; Wei, Y. Syntheses and Properties of Tri- and Multi-Block Copolymers Consisting of Polybutadiene and Polylactide Segments. *RSC Adv.* **2022**, *12* (46), 29777−29784.
(190) Yuntawattana, N.; Gregory, G. L.; Carrodeguas, L. P.; Williams, C. K. Switchable Polymerization Catalysis Using a Tin(II) Catalyst and Commercial Monomers to Toughen Poly(l-Lactide). *ACS Macro Lett.* **2021**, *10* (7), 774−779.
(191) *Council Decision (EU, Euratom) 2020/2053 of 14 December 2020 on the System of Own Resources of the European Union and Repealing Decision 2014/335/EU, Euratom*; 2020; Vol. *424*. http://data.europa.eu/eli/dec/2020/2053/oj/eng (accessed 2024-08-13).
(192) *Directive (EU) 2015/720 of the European Parliament and of the Council of 29 April 2015 Amending Directive 94/62/EC as Regards Reducing the Consumption of Lightweight Plastic Carrier Bags (Text with EEA Relevance)*; 2015; Vol. *115*. http://data.europa.eu/eli/dir/2015/720/oj/eng (accessed 2024-08-13).
(193) *Directive (EU) 2019/904 of the European Parliament and of the Council of 5 June 2019 on the Reduction of the Impact of Certain Plastic Products on the Environment (Text with EEA Relevance)*; 2019; Vol. *155*. http://data.europa.eu/eli/dir/2019/904/oj/eng (accessed 2024-08-13).
(194) *EU Policy Framework on Biobased, Biodegradable and Compostable Plastics*, 2022.
(195) *Regulation (EU) 2024/1781 of the European Parliament and of the Council of 13 June 2024 Establishing a Framework for the Setting of Ecodesign Requirements for Sustainable Products, Amending Directive (EU) 2020/1828 and Regulation (EU) 2023/1542 and Repealing Directive 2009/125/EC (Text with EEA Relevance)*; 2024. http://data.europa.eu/eli/reg/2024/1781/oj/eng (accessed 2024-08-13).
(196) *Plastic Taxation in Europe 2024*; WTS Global, 2023.

https://doi.org/10.1021/acs.biomac.5c00161
Biomacromolecules 2025, 26, 2761−2783

(197) *Promoting Compostable Bioplastics in the APEC Region: Policy Frameworks to Enable Trade, Investment and Innovation*; Asia-Pacific Economic Cooperation, 2024.
(198) *Guide to EPR and Packaging Legislation | EcoEnclose*. https://www.ecoenclose.com/resources/epr-packaging-requirements (accessed 2024-08-13).
(199) *Packaging EPR Laws in the U.S. Source Intelligence*. https://blog.sourceintelligence.com/packaging-epr-laws-in-the-us (accessed 2024-11-25).
(200) *Bold Goals for U.S. Biotechnology and Manufacturing: Harnessing Research and Development to Further Societal Goals*; The White House, 2023.
(201) *Building a Resilient Biomass Supply: A Plan to Enable the Bioeconomy in America*; The White House, 2024.
(202) *Standard Test Method for Determining Aerobic Biodegradation of Plastic Materials Under Controlled Composting Conditions, Incorporating Thermophilic Temperatures*; ASTM International, 2021. DOI: 10.1520/D5338-15R21.
(203) Standard Specification for Labeling of Plastics Designed to Be Aerobically Composted in Municipal or Industrial Facilities, 2023. DOI: 10.1520/D6400-23.
(204) *Standard Specification for Labeling of End Items That Incorporate Plastics and Polymers as Coatings or Additives with Paper and Other Substrates Designed to Be Aerobically Composted in Municipal or Industrial Facilities*; ASTM International, 2021. DOI: 10.1520/D6868-21.
(205) *EN 13432 Certified Bioplastics: Performance in Industrial Composting*; European Bioplastics, 2015.
(206) Le Pera, A.; Sellaro, M.; Sicilia, F.; Ciccoli, R.; Sceberras, B.; Freda, C.; Fanelli, E.; Cornacchia, G. Environmental and Economic Impacts of Improper Materials in the Recycling of Separated Collected Food Waste through Anaerobic Digestion and Composting. *Sci. Total Environ.* **2023**, *880*, No. 163240.
(207) Colombini, G.; Rumpel, C.; Houot, S.; Biron, P.; Dignac, M.-F. A Long-Term Field Experiment Confirms the Necessity of Improving Biowaste Sorting to Decrease Coarse Microplastic Inputs in Compost Amended Soils. *Environ. Pollut.* **2022**, *315*, No. 120369.
(208) Wang, Q.; Adams, C. A.; Wang, F.; Sun, Y.; Zhang, S. Interactions between microplastics and soil fauna: A critical review. *Critical Reviews in Environmental Science and Technology* **2022**, *52* (18), 3211−3243.
(209) Benavides, P. T.; Lee, U.; Zarè-Mehrjerdi, O. Life Cycle Greenhouse Gas Emissions and Energy Use of Polylactic Acid, Bio-Derived Polyethylene, and Fossil-Derived Polyethylene. *J. Clean. Prod.* **2020**, *277*, No. 124010.
(210) Krause, M. J.; Townsend, T. G. Life-Cycle Assumptions of Landfilled Polylactic Acid Underpredict Methane Generation. *Environ. Sci. Technol. Lett.* **2016**, *3* (4), 166−169.
(211) Vink, E. T. H.; Davies, S. Life Cycle Inventory and Impact Assessment Data for 2014 Ingeo Polylactide Production. *Ind. Biotechnol.* **2015**, *11* (3), 167−180.
(212) Brizga, J.; Hubacek, K.; Feng, K. The Unintended Side Effects of Bioplastics: Carbon, Land, and Water Footprints. *One Earth* **2020**, *3* (1), 45−53.
(213) *PVC price index*. businessanalytiq. https://businessanalytiq.com/procurementanalytics/index/pvc-price-index/ (accessed 2025-01-17).
(214) *PET (Polyethylene Terephthalate) price index*. businessanalytiq. https://businessanalytiq.com/procurementanalytics/index/pet-price-index/ (accessed 2025-01-17).
(215) *HDPE price index*. businessanalytiq. https://businessanalytiq.com/procurementanalytics/index/hdpe-price-index/ (accessed 2025-01-17).
(216) *Polypropylene price index*. businessanalytiq. https://businessanalytiq.com/procurementanalytics/index/polypropylene-price-index/ (accessed 2025-01-17).
(217) *Polystyrene (PS) price index*. businessanalytiq. https://businessanalytiq.com/procurementanalytics/index/polystyrene-ps-price-index/ (accessed 2025-01-17).
(218) *Polylactic acid (PLA) price index*. businessanalytiq. https://businessanalytiq.com/procurementanalytics/index/polylactic-acid-pla-price-index/ (accessed 2025-01-17).
(219) Filho, W. L.; Barbir, J.; Abubakar, I. R.; Paco, A.; Stasiskiene, Z.; Hornbogen, M.; Christin Fendt, M. T.; Voronova, V.; Kloga, M. Consumer Attitudes and Concerns with Bioplastics Use: An International Study. *PLoS One* **2022**, *17* (4), No. e0266918.
(220) Zwicker, M. V.; Brick, C.; Gruter, G.-J. M.; van Harreveld, F. Consumer Attitudes and Willingness to Pay for Novel Bio-Based Products Using Hypothetical Bottle Choice. *Sustain. Prod. Consum.* **2023**, *35*, 173−183.
(221) Zhou, C.; Wang, Y. Recent Progress in the Conversion of Biomass Wastes into Functional Materials for Value-Added Applications. *Sci. Technol. Adv. Mater.* **2020**, *21* (1), 787−804.
(222) Arora, Y.; Sharma, S.; Sharma, V. Microalgae in Bioplastic Production: A Comprehensive Review. *Arab. J. Sci. Eng.* **2023**, *48* (6), 7225−7241.
(223) Maraveas, C. Production of Sustainable and Biodegradable Polymers from Agricultural Waste. *Polymers* **2020**, *12* (5), 1127.
(224) da Silva, S. A.; Hinkel, E. W.; Lisboa, T. C.; Selistre, V. V.; da Silva, A. J.; da Silva, L. O. F.; Faccin, D. J. L.; Cardozo, N. S. M. A Biostimulation-Based Accelerated Method for Evaluating the Biodegradability of Polymers. *Polym. Test.* **2020**, *91*, No. 106732.
(225) Gu, Z.; Zhang, J.; Cao, W.; Liu, X.; Wang, J.; Zhang, X.; Chen, W.; Bao, J. Extraordinary Toughness and Heat Resistance Enhancement of Biodegradable PLA/PBS Blends through the Formation of a Small Amount of Interface-Localized Stereocomplex Crystallites during Melt Blending. *Polymer* **2022**, *262*, No. 125454.
(226) Hsieh, H. L. Industrial Applications of Anionic Polymerization: An Introduction. In *Applications of Anionic Polymerization Research*; ACS Symposium Series; American Chemical Society, 1998; Vol. *696*, pp 28−33. DOI: 10.1021/bk-1998-0696.ch002.
(227) *Anionic Polymerization: Principles, Practice, Strength, Consequences and Applications*; Hadjichristidis, N., Hirao, A., Eds.; Springer Japan: Tokyo, 2015. DOI: 10.1007/978-4-431-54186-8.
(228) Albalak, R. *Polymer Devolatilization*; Routledge, 2017.
(229) McGuire, T. M.; Buchard, A.; Williams, C. Chemical Recycling of Commercial Poly(l-Lactic Acid) to l-Lactide Using a High-Performance Sn(II)/Alcohol Catalyst System. *J. Am. Chem. Soc.* **2023**, *145* (36), 19840−19848.
(230) Lou, X.; Detrembleur, C.; Jérôme, R. Living Cationic Polymerization of δ-Valerolactone and Synthesis of High Molecular Weight Homopolymer and Asymmetric Telechelic and Block Copolymer. *Macromolecules* **2002**, *35* (4), 1190−1195.
(231) Shibasaki, Y.; Sanada, H.; Yokoi, M.; Sanda, F.; Endo, T. Activated Monomer Cationic Polymerization of Lactones and the Application to Well-Defined Block Copolymer Synthesis with Seven-Membered Cyclic Carbonate. *Macromolecules* **2000**, *33* (12), 4316−4320.
(232) Ren, Q.; Wu, M.; Wang, L.; Zheng, W.; Hikima, Y.; Semba, T.; Ohshima, M. Cellulose Nanofiber Reinforced Poly (Lactic Acid) with Enhanced Rheology, Crystallization and Foaming Ability. *Carbohydr. Polym.* **2022**, *286*, No. 119320.
(233) Kelly, P. V.; Shams Es-haghi, S.; Ahmad, A. A. L.; Lamm, M. E.; Copenhaver, K.; Alyamac-Seydibeyoglu, E.; Ozcan, S.; Gardner, D. J.; Gramlich, W. M. High-Strength 3D Printed Poly(Lactic Acid) Composites Reinforced by Shear-Aligned Polymer-Grafted Cellulose Nanofibrils. *RSC Appl. Polym.* **2025**, *3* (1), 111−124.
(234) Qian, K.; Qian, X.; Chen, Y.; Zhou, M. Poly(Lactic Acid)−Thermoplastic Poly(Ether)Urethane Composites Synergistically Reinforced and Toughened with Short Carbon Fibers for Three-Dimensional Printing. *J. Appl. Polym. Sci.* **2018**, *135* (29), No. 46483.
(235) Münstedt, H.; Kurzbeck, S.; Stange, J. Importance of Elongational Properties of Polymer Melts for Film Blowing and Thermoforming. *Polym. Eng. Sci.* **2006**, *46* (9), 1190−1195.
(236) Dealy, J. M.; Read, D. J.; Larson, R. G. Structure and Rheology of Molten Polymers. In *Structure and Rheology of Molten Polymers*; Carl Hanser Verlag GmbH & Co. KG, 2018; p I−XVII. DOI: 10.3139/9781569906125.fm.

(237) López-Barrón, C. R.; Tsou, A. H. Strain Hardening of Polyethylene/Polypropylene Blends via Interfacial Reinforcement with Poly(Ethylene-Cb-Propylene) Comb Block Copolymers. *Macromolecules* **2017**, *50* (7), 2986−2995.
(238) López-Barrón, C. R.; Brant, P.; Shivokhin, M.; Lu, J.; Kang, S.; Throckmorton, J. A.; Mouton, T.; Pham, T.; Savage, R. C. Long-Chain Hyperbranched Comb Block Copolymers: Synthesis, Microstructure, Rheology, and Thermal Behavior. *Macromolecules* **2018**, *51* (15), 5720−5731.
(239) Jiang, Y.; Yan, C.; Shi, D.; Liu, Z.; Yang, M. Enhanced Rheological Properties of PLLA with a Purpose-Designed PDLA-b-PEG-b-PDLA Triblock Copolymer and the Application in the Film Blowing Process to Acquire Biodegradable PLLA Films. *ACS Omega* **2019**, *4* (8), 13295−13302.
(240) Quynh, T. M.; Mai, H. H.; Lan, P. N. Stereocomplexation of Low Molecular Weight Poly(L-Lactic Acid) and High Molecular Weight Poly(D-Lactic Acid), Radiation Crosslinking PLLA/PDLA Stereocomplexes and Their Characterization. *Radiat. Phys. Chem.* **2013**, *83*, 105−110.
(241) Tsuji, H. In Vitro Hydrolysis of Blends from Enantiomeric Poly(Lactide)s. Part 4: Well-Homo-Crystallized Blend and Non-blended Films. *Biomaterials* **2003**, *24* (4), 537−547.
(242) Zhang, X.; Yang, B.; Fan, B.; Sun, H.; Zhang, H. Enhanced Nonisothermal Crystallization and Heat Resistance of Poly(l-Lactic Acid) by d-Sorbitol as a Homogeneous Nucleating Agent. *ACS Macro Lett.* **2021**, *10* (1), 154−160.
(243) Shi, K.; Liu, G.; Sun, H.; Yang, B.; Weng, Y. Effect of Biomass as Nucleating Agents on Crystallization Behavior of Polylactic Acid. *Polymers* **2022**, *14* (20), 4305.
(244) *Standard Test Method for Deflection Temperature of Plastics Under Flexural Load in the Edgewise Position*; ASTM International, 2018.
(245) *Standard Test Method for Distortion Temperature in Three-Point Bending by Thermomechanical Analysis*; ASTM International, 2023.
(246) *Standard Test Method for Vicat Softening Temperature of Plastics*; ASTM International, 2017.
(247) Tábi, T.; Hajba, S.; Kovács, J. G. Effect of Crystalline Forms (A′ and α) of Poly(Lactic Acid) on Its Mechanical, Thermo-Mechanical, Heat Deflection Temperature and Creep Properties. *Eur. Polym. J.* **2016**, *82*, 232−243.
(248) Wang, W.; Lu, W.; Goodwin, A.; Wang, H.; Yin, P.; Kang, N.-G.; Hong, K.; Mays, J. W. Recent Advances in Thermoplastic Elastomers from Living Polymerizations: Macromolecular Architectures and Supramolecular Chemistry. *Prog. Polym. Sci.* **2019**, *95*, 1−31.
(249) Rutala, W. A.; Weber, D. J. *Guideline for Disinfection and Sterilization in Healthcare Facilities, 2008 (Update June 2024)*; Center for Disease Control, 2023. https://www.cdc.gov/infection-control/hcp/disinfection-sterilization/ethylene-oxide-sterilization.html?CDC_AAref_Val=https://www.cdc.gov/infectioncontrol/guidelines/disinfection/sterilization/ethylene-oxide.html.
(250) Hutchinson, J. M. Physical Aging of Polymers. *Prog. Polym. Sci.* **1995**, *20* (4), 703−760.
(251) Pan, P.; Zhu, B.; Inoue, Y. Enthalpy Relaxation and Embrittlement of Poly(l-Lactide) during Physical Aging. *Macromolecules* **2007**, *40* (26), 9664−9671.
(252) Lin, Y.; Cao, J.; Zhu, M.; Bilotti, E.; Zhang, H.; Bastiaansen, C. W. M.; Peijs, T. High-Performance Transparent Laminates Based on Highly Oriented Polyethylene Films. *ACS Appl. Polym. Mater.* **2020**, *2* (6), 2458−2468.
(253) Lee, S. J.; Jeoung, H. G.; Ahn, K. H. Influence of Solvent Contents on the Rubber-Phase Particle Size Distribution of High-Impact Polystyrene. *J. Appl. Polym. Sci.* **2003**, *89* (13), 3672−3679.
(254) Xu, L.; Tang, Q.; Liu, B.; Zhang, M. Control of the Composition of Matrix Resin for the Design of MABS Resin with Good Transparency and Toughness. *Colloids Surf. Physicochem. Eng. Asp.* **2023**, *658*, No. 130608.
(255) Borrelle, S. B.; Ringma, J.; Law, K. L.; Monnahan, C. C.; Lebreton, L.; McGivern, A.; Murphy, E.; Jambeck, J.; Leonard, G. H.; Hilleary, M. A.; Eriksen, M.; Possingham, H. P.; De Frond, H.; Gerber, L. R.; Polidoro, B.; Tahir, A.; Bernard, M.; Mallos, N.; Barnes, M.; Rochman, C. M. Predicted Growth in Plastic Waste Exceeds Efforts to Mitigate Plastic Pollution. *Science* **2020**, *369* (6510), 1515−1518.
(256) Lau, W. W. Y.; Shiran, Y.; Bailey, R. M.; Cook, E.; Stuchtey, M. R.; Koskella, J.; Velis, C. A.; Godfrey, L.; Boucher, J.; Murphy, M. B.; Thompson, R. C.; Jankowska, E.; Castillo Castillo, A.; Pilditch, T. D.; Dixon, B.; Koerselman, L.; Kosior, E.; Favoino, E.; Gutberlet, J.; Baulch, S.; Atreya, M. E.; Fischer, D.; He, K. K.; Petit, M. M.; Sumaila, U. R.; Neil, E.; Bernhofen, M. V.; Lawrence, K.; Palardy, J. E. Evaluating Scenarios toward Zero Plastic Pollution. *Science* **2020**, *369* (6510), 1455−1461.

https://doi.org/10.1021/acs.biomac.5c00161
Biomacromolecules 2025, 26, 2761−2783